

Supporting Information

Synthesis and structural diversity of trivalent rare-earth metal diisopropylamide complexes

Tatiana Spallek,^a Oliver Heß,^a Melanie Meermann-Zimmermann,^b Christian Meermann,^a Michael G. Klimpel,^c Frank Estler,^c David Schneider,^a Wolfgang Scherer,^d Maxim Tafipolsky,^{c,d} Karl W. Törnroos,^b Cäcilia Maichle-Mössmer,^a Peter Sirsch^{a,*} and Reiner Anwander^{a,*}

^a Institut für Anorganische Chemie, Universität Tübingen, Auf der Morgenstelle 18, 72076 Tübingen, Germany. E-mail: reiner.anwander@uni-tuebingen.de, peter.sirsch@uni-tuebingen.de

^b Department of Chemistry, University of Bergen, Allégaten 41, 5007 Bergen, Norway

^c Anorganisch-chemisches Institut, Technische Universität München, Lichtenbergstraße 4, 85747 Garching, Germany

^d Institut für Physik, Universität Augsburg, Universitätsstraße 1, D-86159 Augsburg, Germany

X-Ray Crystallographic data

Figure S1. Molecular structure of LiY(NiPr ₂) ₄ (THF) (1b)	S4
Figure S2. Molecular structure of LiLa(NiPr ₂) ₄ (THF) (1c)	S4
Figure S3. Molecular structure of NaSc(NiPr ₂) ₄ (THF) (2a)	S5
Figure S4. Molecular structure of NaY(NiPr ₂) ₄ (THF) (2b)	S5
Figure S5. Molecular structure of NaLu(NiPr ₂) ₄ (THF) (2d)	S6
Figure S6. Asymmetric unit of the crystal structure of LiSc(NiPr ₂) ₄ (THF) (1a)	S6
Figure S7. Molecular structure of NaSc(NiPr ₂) ₄ (THF) ₂ (3a)	S7
Figure S8. Molecular structure of NaLa(NiPr ₂) ₄ (THF) ₂ (3c)	S7
Figure S9. Molecular structure of [Lu(NiPr ₂) ₂ (THF)(μ-Cl)] ₂ (5d)	S8
Figure S10. Asymmetric unit of the crystal structure of [Y(NiPr ₂) ₂ (THF)(μ-Cl)] ₂ (5b)	S8
Figure S11. Disorder model for complex [La(NiPr ₂) ₂ (THF)(μ-Cl)] ₂ × La(NiPr ₂) ₃ (THF) ₂ (5c')	S9
Figure S12. Molecular structure of Lu(NiPr ₂) ₂ Cl(THF) ₂ (7b)	S9
Table S1. Summary of crystallographic data for compounds 1a – d	S10
Table S2. Summary of crystallographic data for compounds 2a, 2b , and 2d .	S10
Table S3. Summary of crystallographic data for compounds 3a – c , and 4a	S11
Table S4. Summary of crystallographic data for compounds 5a, 5b, 5c' , and 5d	S11
Table S5. Summary of crystallographic data for compounds 6 and 7a - b	S12
Table S6. Summary of crystallographic data for compounds 8, 9 , and 10	S12

NMR spectroscopic data

Figure S13. ¹ H NMR spectrum of LiSc(NiPr ₂) ₄ (THF) (1a)	S13
Figure S14. ¹ H NMR spectrum of LiY(NiPr ₂) ₄ (THF) (1b)	S13
Figure S15. VT ¹ H NMR spectra of LiY(NiPr ₂) ₄ (THF) (1b)	S14
Figure S16. ¹ H- ¹³ C HSQC NMR spectrum of LiY(NiPr ₂) ₄ (THF) (1b)	S14
Figure S17. ¹³ C -coupled ¹ H NMR spectrum of LiY(NiPr ₂) ₄ (THF) (1b)	S15
Figure S18. VT ¹ H NMR spectra of LiLa(NiPr ₂) ₄ (THF) (1c)	S15
Figure S19. VT ¹ H NMR spectra of NaY(NiPr ₂) ₄ (THF) (2b)	S16
Figure S20. ¹ H NMR spectrum of NaLu(NiPr ₂) ₄ (THF) (2d)	S16
Figure S21. ¹³ C NMR spectrum of NaLu(NiPr ₂) ₄ (THF) (2d)	S17
Figure S22. ¹ H NMR spectrum of NaY(NiPr ₂) ₄ (THF) ₂ (3b)	S17
Figure S23. ¹³ C NMR spectrum of NaY(NiPr ₂) ₄ (THF) ₂ (3b)	S18
Figure S24. ¹ H NMR spectrum of Sc(NiPr ₂) ₃ (THF) (4a)	S18
Figure S25. ¹ H NMR spectrum of Sc[(NiPr ₂) ₂ (THF)(μ-Cl)] ₂ (5a)	S19
Figure S26. ¹ H NMR spectrum of Y[(NiPr ₂) ₂ (THF)(μ-Cl)] ₂ (5b)	S19
Figure S27. ¹ H NMR spectrum of La(NiPr ₂) ₂ (THF)(μ-Cl) × La(NiPr ₂) ₃ (THF) ₂ (5c')	S20
Figure S28. ¹ H NMR spectrum of Lu[(NiPr ₂) ₂ (THF)(μ-Cl)] ₂ (5d)	S20
Figure S29. ¹ H NMR spectrum of La(NiPr ₂) ₃ (THF) ₂ (6)	S21
Figure S30. ¹ H NMR spectrum of Sc(NiPr ₂) ₂ Cl(THF) ₂ (7a)	S21
Figure S31. ¹ H NMR spectrum of Lu(NiPr ₂) ₂ Cl(THF) ₂ (7b)	S22
Figure S32. ¹ H NMR spectrum of [LiY(NiPr ₂) ₄] _n (8)	S22
Figure S33. ¹ H NMR spectrum of [LiY(NiPr ₂) ₄] _n (8)	S23
Figure S34. VT ¹ H NMR spectra of [LiY(NiPr ₂) ₄] _n (8)	S23
Figure S35. ¹³ C NMR spectrum of [LiY(NiPr ₂) ₄] _n (8)	S24
Figure S36. ¹ H NMR spectrum of {[Sc(NiPr ₂)Cl ₂ (THF)] ₂ (LiCl)} ₂ (9)	S24
Figure S37. ¹ H NMR spectrum of [Sc(NiPr ₂)Cl ₂ (THF)] ₄ (10)	S25

DFT Calculations

Figure S38. DFT-optimised geometry and selected geometrical parameters of 1a'	S26
Figure S39. DFT-optimised geometry and selected geometrical parameters of 1a''	S26
Table S7. Selected geometrical parameters of 1a''	S27
Table S8. Cartesian Coordinates of 1a'	S27
Table S9. Cartesian Coordinates of 1a''	S29

X-Ray Crystallographic data

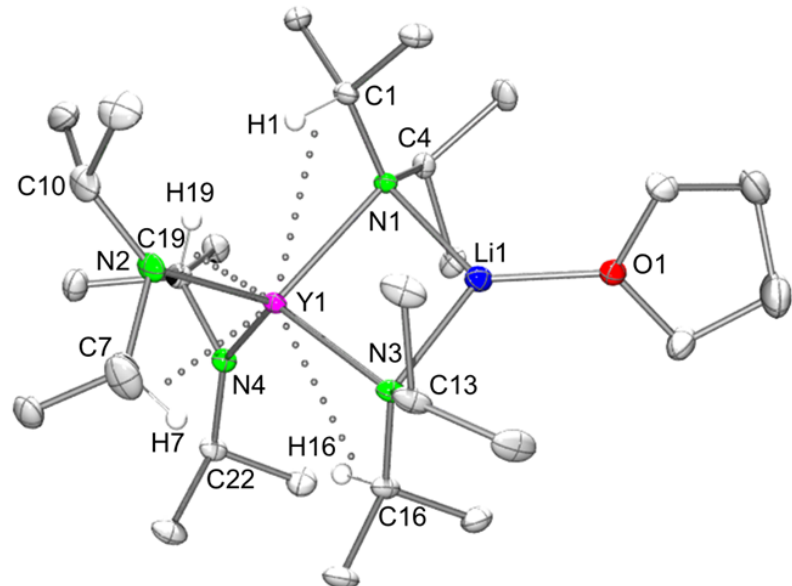


Figure S1. Molecular structure of $\text{LiY}(\text{NiPr}_2)_4(\text{THF})$ (**1b**). Non-hydrogen atoms are represented by atomic displacement ellipsoids at the 30% level. Hydrogen atoms are omitted for clarity, except those showing close metal contacts.

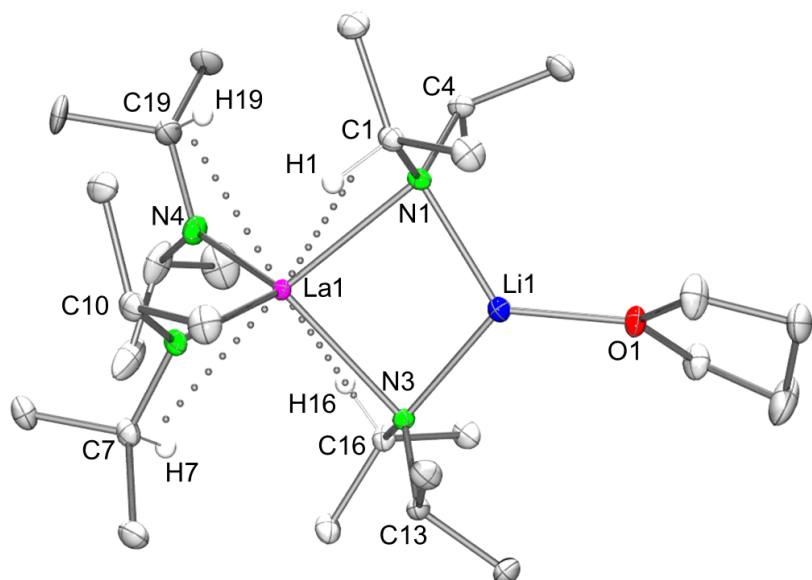


Figure S2. Molecular structure of $\text{LiLa}(\text{NiPr}_2)_4(\text{THF})$ (**1c**). Non-hydrogen atoms are represented by atomic displacement ellipsoids at the 30% level. Hydrogen atoms are omitted for clarity, except those showing close metal contacts.

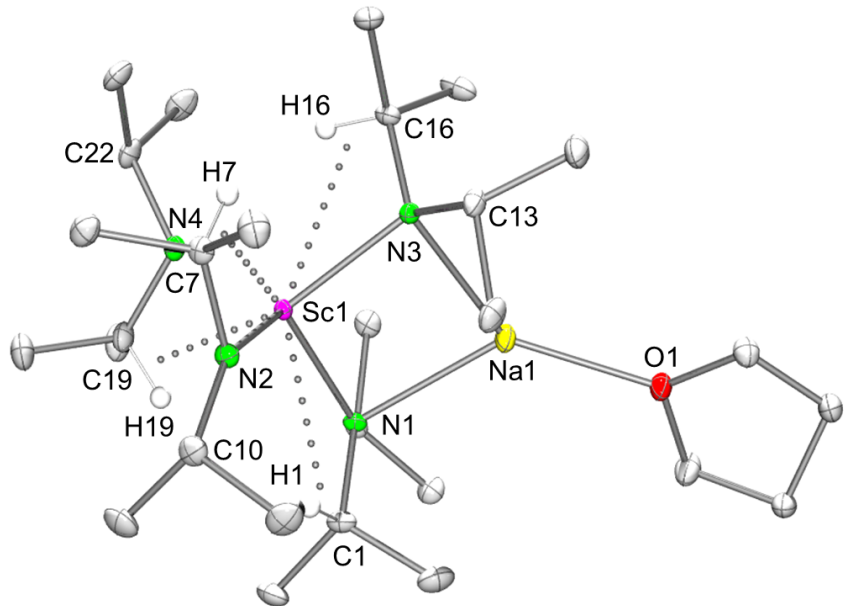


Figure S3. Molecular structure of $\text{NaSc}(\text{NiPr}_2)_4(\text{THF})$ (**2a**). Non-hydrogen atoms are represented by atomic displacement ellipsoids at the 30% level. Hydrogen atoms are omitted for clarity, except those showing close metal contacts.

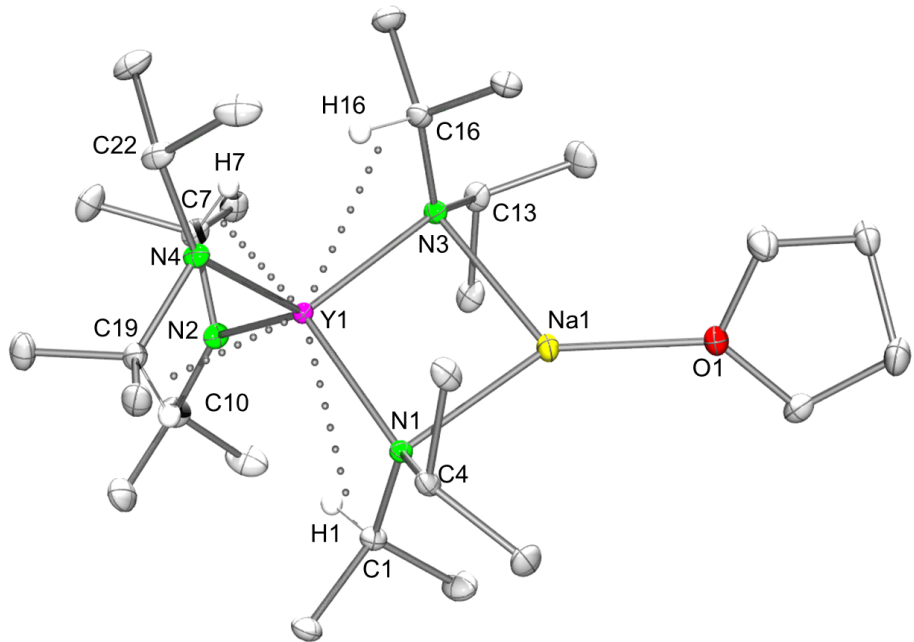


Figure S4. Molecular structure of $\text{NaY}(\text{NiPr}_2)_4(\text{THF})$ (**2b**). Non-hydrogen atoms are represented by atomic displacement ellipsoids at the 30% level. Hydrogen atoms are omitted for clarity, except those showing close metal contacts.

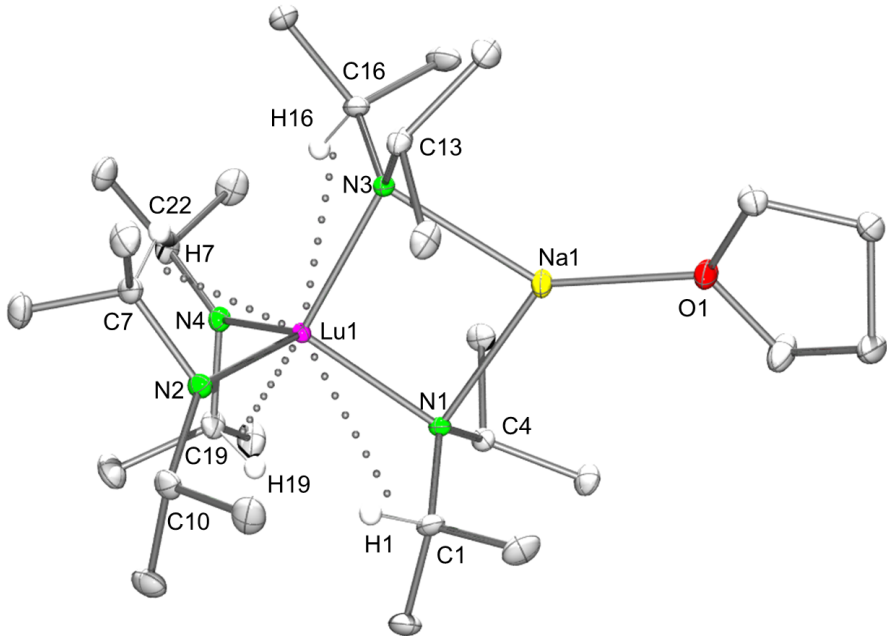


Figure S5. Molecular structure of $\text{NaLu}(\text{NiPr}_2)_4(\text{THF})$ (**2d**). Non-hydrogen atoms are represented by atomic displacement ellipsoids at the 30% level. Hydrogen atoms are omitted for clarity, except those showing close metal contacts.

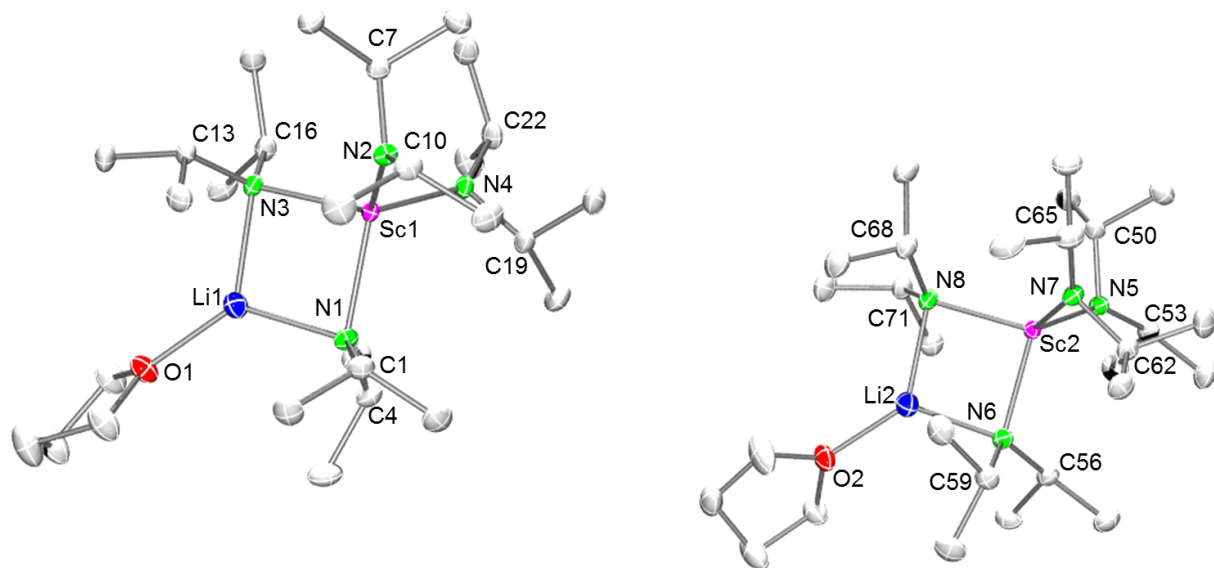


Figure S6. Asymmetric unit of the crystal structure of $\text{AMLn}(\text{NiPr}_2)_4(\text{THF})$ (AM = Li; Ln = Sc (**1a**), Y (**1b**), La (**1c**), Lu (**1d**); AM = Na; Ln = Sc (**2a**), Y (**2b**), Lu (**2d**)), representatively shown for $\text{LiSc}(\text{NiPr}_2)_4(\text{THF})$ (**1a**). Non-hydrogen atoms are represented by atomic displacement ellipsoids at the 50% level. Hydrogen atoms are omitted for clarity.

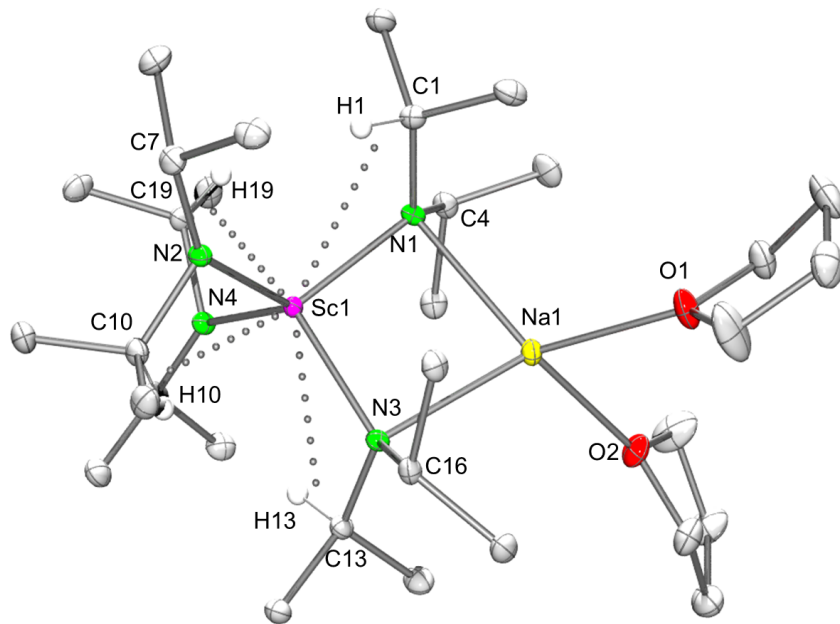


Figure S7. Molecular structure of $\text{NaSc}(\text{NiPr}_2)_4(\text{THF})_2$ (**3a**). Non-hydrogen atoms are represented by atomic displacement ellipsoids at the 30% level. Hydrogen atoms are omitted for clarity, except those showing close metal contacts.

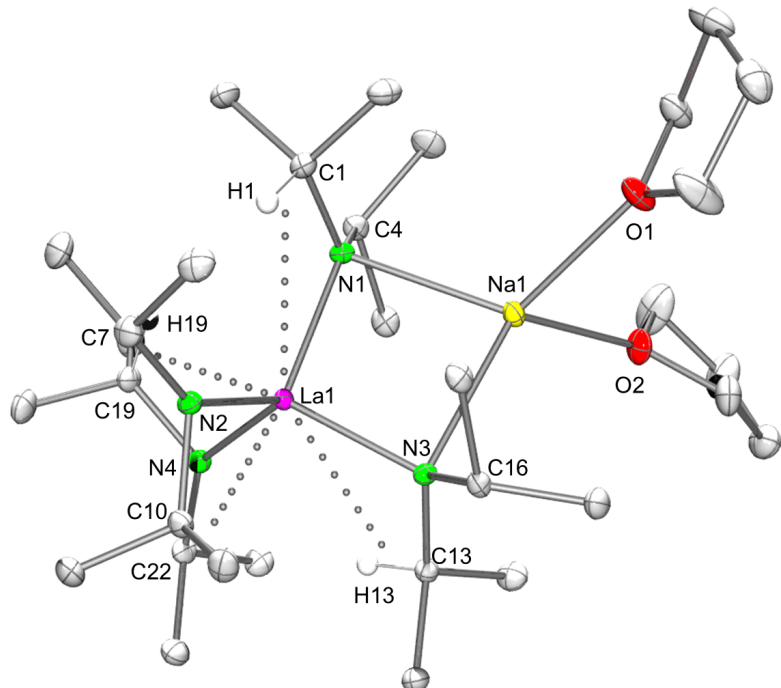


Figure S8. Molecular structure of $\text{NaLa}(\text{NiPr}_2)_4(\text{THF})_2$ (**3c**). Non-hydrogen atoms are represented by atomic displacement ellipsoids at the 30% level. Hydrogen atoms are omitted for clarity, except those showing close metal contacts.

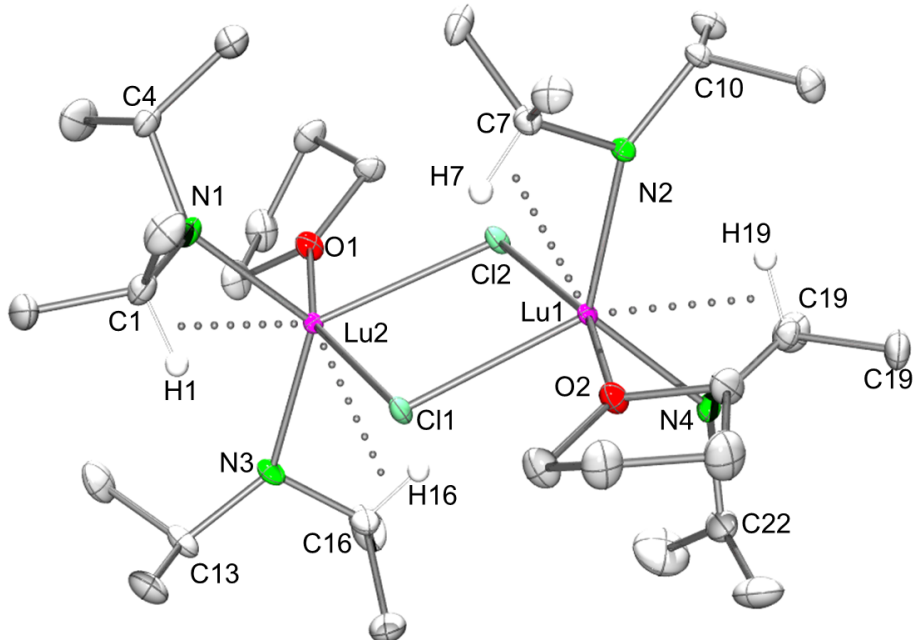


Figure S9. Molecular structure of $[\text{Lu}(\text{NiPr}_2)_2(\text{THF})(\mu\text{-Cl})]_2$ (**5d**). Non-hydrogen atoms are represented by atomic displacement ellipsoids at the 30% level. Hydrogen atoms are omitted for clarity, except those showing close metal contacts.

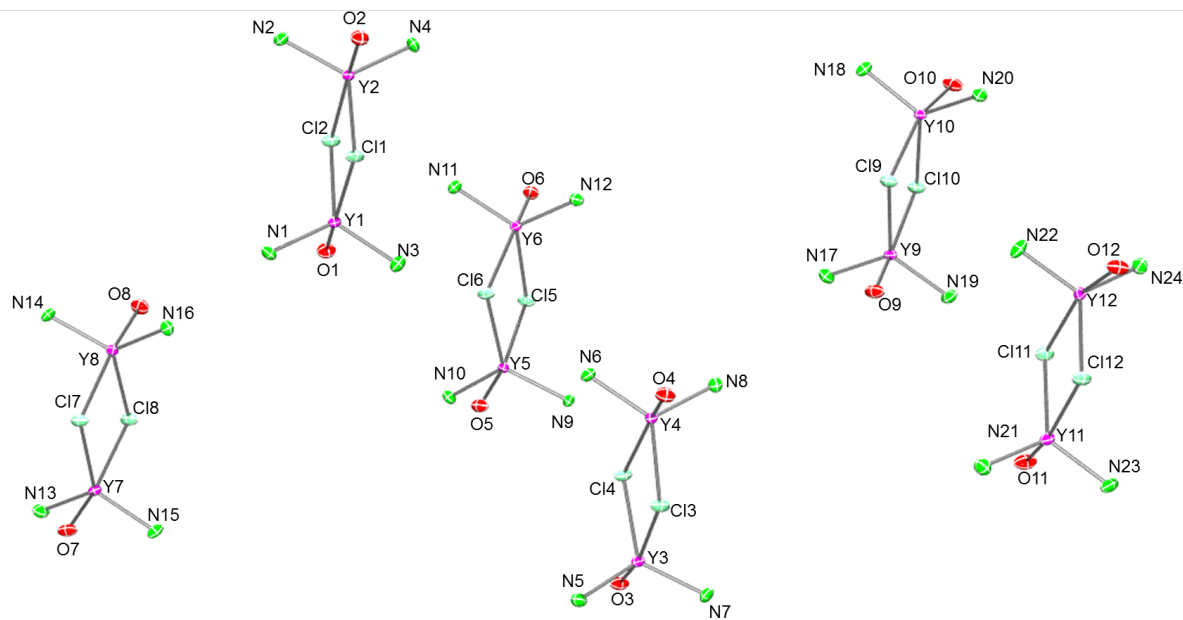


Figure S10. Asymmetric unit of the crystal structure of complexes $[\text{Ln}(\text{NiPr}_2)_2(\text{THF})(\mu\text{-Cl})]_2$ ($\text{Ln} = \text{Sc}$ (**5a**), Y (**5b**), and Lu (**5d**))), representatively shown for the yttrium derivative **5b**. Non-carbon and non-hydrogen atoms are represented by atomic displacement ellipsoids at the 50% level. Carbon and hydrogen atoms are omitted for clarity.

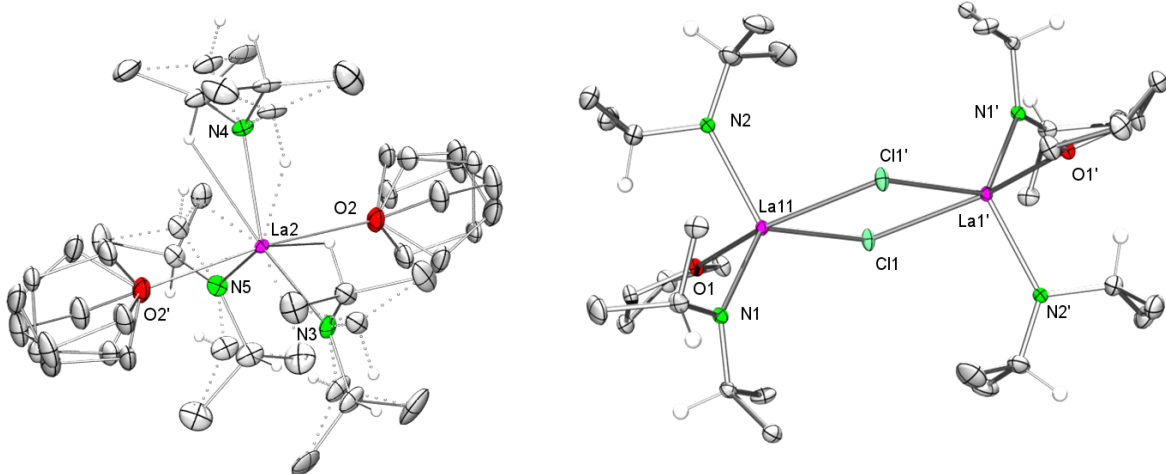


Figure S11. Disorder model for complex $[\text{La}(\text{NiPr}_2)_2(\text{THF})(\mu\text{-Cl})]_2 \times \text{La}(\text{NiPr}_2)_3(\text{THF})_2$ (**5c'**). Part 2 (left) features a disorder of the amido ligands, where the two components show either a clockwise or anticlockwise orientation for the hydrogen atoms on the tertiary carbon atoms. An additional disorder about the inversion center is omitted for clarity.

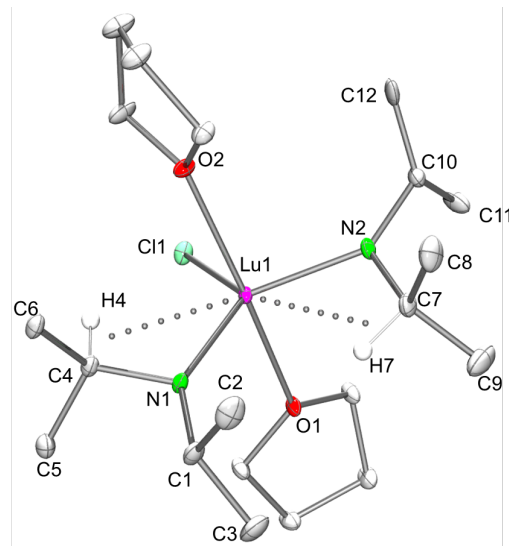


Figure S12. Molecular structure of $\text{Lu}(\text{NiPr}_2)_2\text{Cl}(\text{THF})_2$ (**7b**). Non-hydrogen atoms are represented by atomic displacement ellipsoids at the 30% level. Hydrogen atoms are omitted for clarity, except those showing close metal contacts.

For all obtained Data:

$$^a R_1 = \frac{\sum(|F_0| - |F_c|)}{\sum|F_0|}, F_0 > 4\sigma(F_0)$$

$$^b wR_2 = \left\{ \sum w(F_0^2 - F_c^2)^2 / \sum w(F_0^2)^2 \right\}^{1/2}$$

$$^c GOF = \left[\sum w(F_0^2 - F_c^2)^2 / (n_0 - n_p) \right]^{1/2}$$

Table S1. Summary of crystallographic data for compounds **1a – d**

	1a	1b	1c	1d
Formula	C ₂₈ H ₆₄ LiN ₄ OSc	C ₂₈ H ₆₄ LiN ₄ OY	C ₂₈ H ₆₄ LaLiN ₄ O	C ₂₈ H ₆₄ LiLuN ₄ O
Fw [g/mol]	524.73	568.68	618.68	654.74
T [K]	100(2)	100(2)	100(2)	100(2)
cryst. system	monoclinic	Monoclinic	monoclinic	monoclinic
space group	P21/c	P21/c	P21/c	P21/c
a [Å]	14.9737(3)	15.2060(6)	15.1993(11)	15.0828(9)
b [Å]	21.2886(4)	21.1050(7)	21.2350(14)	21.3232(13)
c [Å]	20.7196(4)	21.0749(8)	21.2895(14)	20.9299(14)
β [°]	92.3560(10)	94.0690(10)	95.637(4)	92.885(2)
Volume [Å³]	6599.2(2)	6746.4(4)	6838.1(8)	6722.8(7)
Z	8	8	8	8
ρ_{calcd} [mg/m³]	1.056	1.120	1.202	1.294
μ [mm⁻¹]	0.247	1.752	1.272	2.960
R₁^a [I > 2.0 σ(I)]	0.0387	0.0352	0.0235	0.0216
wR₂^b (all data)	0.1006	0.0782	0.0514	0.0477
GOF^c	0.994	1.022	1.043	1.020
CCDC	1471684	1471680	1471683	1471682

Table S2. Summary of crystallographic data for compounds **2a**, **2b**, and **2d**. For **2c**, the unit cell only was determined, which is isotropic

	2a	2b	2c	2d
Formula	C ₂₈ H ₆₄ N ₄ NaOSc	C ₂₈ H ₆₄ N ₄ NaOY	C ₂₈ H ₆₄ N ₄ NaOLa	C ₂₈ H ₆₄ LuN ₄ NaO
Fw [g/mol]	540.78	584.73	634.74	670.79
T [K]	100(2)	100(2)	100(2)	108(2)
cryst. system	monoclinic	monoclinic	monoclinic	monoclinic
space group	P21/c	P21/c	P21/c	P21/c
a [Å]	15.7249(3)	15.7168(3)	15.676(9)	15.7468(6)
b [Å]	20.4979(4)	20.7661(5)	21.128(12)	20.6709(7)
c [Å]	20.6858(4)	20.9724(5) Å	21.271(12)	20.8642(7)
β [°]	93.6700(10)	93.7880(10)	94.235(5)	93.719(2)
Volume [Å³]	6653.9(2)	6829.9(3)	-	6777.0(4)
Z	8	8	-	8
ρ_{calcd} [mg/m³]	1.080	1.137	-	1.315
μ [mm⁻¹]	0.258	1.744	-	2.950
R₁^a [I > 2.0 σ(I)]	0.0455	0.0374	-	0.0195
wR₂^b (all data)	0.1015	0.0778	-	0.0447
GOF^c	1.024	1.018	-	1.023
CCDC	1471676	1471681		1471678

Table S3. Summary of crystallographic data for compounds **3a – c** and **4a**

	3a	3b	3c	4a
Formula	C ₃₂ H ₇₂ N ₄ NaO ₂ Sc	C ₃₂ H ₇₂ N ₄ NaO ₂ Y	C ₃₂ H ₇₂ N ₄ NaO ₂ La	C ₂₂ H ₅₀ N ₃ OSc
Fw [g/mol]	612.88	656.83	706.83	417.61
T [K]	100(2)	100(2)	100(2)	100(2)
cryst. system	orthorhombic	orthorhombic	orthorhombic	Monoclinic
space group	P 21 21 21	P 21 21 21	P 21 21 21	P 21/c
a [Å]	12.8672(5)	13.0168(2)	13.1495(9)	17.7101(4)
b [Å]	14.8525(5)	15.0106(3)	15.1703(10)	9.6679(2)
c [Å]	19.3804(7)	19.3492(4)	19.3237(13)	17.0078(4)
β [°]	90	90	90	116.2110(10)
Volume [Å³]	3703.8(2)	3780.64(12)	3854.7(4)	2612.63(10)
Z	4	4	4	4
ρ_{calcd} [mg/m³]	1.099	1.154	1.218	1.062
μ [mm⁻¹]	0.241	1.584	1.149	0.296
R₁^a [I > 2.0 σ(I)]	0.0402	0.0215	0.0266	0.0291
wR₂^b (all data)	0.0876	0.0510	0.0502	0.0797
GOF^c	1.019	1.004	1.032	1.027
CCDC	1471674	1471679	1471677	1471671

Table S4. Summary of crystallographic data for compounds **5a**, **5b**, **5c'**, and **5d**

	5a^a	5b	5c'	5d
Formula	C ₃₂ H ₇₂ Cl ₂ N ₄ O ₂ Sc ₂	C ₃₂ H ₇₂ Cl ₂ N ₄ O ₂ Y ₂	C ₅₈ H ₁₃₀ Cl ₂ La ₃ N ₇ O ₄	C ₃₂ H ₇₂ Cl ₂ Lu ₂ N ₄ O ₂
Fw [g/mol]	705.77	793.66	1477.31	965.78
T [K]	100(2)	100(2)	173(2)	100(2)
cryst. system	Monoclinic	Monoclinic	Monoclinic	Monoclinic
space group	Pc	Pc	P 21/c	Pc
a [Å]	13.4147(3)	13.4201(6)	21.3309(5)	13.5111(3)
b [Å]	29.0755(6)	29.0650(14)	10.6805(3)	28.9345(6)
c [Å]	32.2627(6)	32.2640(15)	16.5145(4)	32.5140(7)
β [°]	100.683(1)	100.720(2)	101.8300(10)	100.5440(10)
Volume [Å³]	-	12365.1(10)	3682.50(16)	12496.3(5)
Z	-	12	2	12
ρ_{calcd} [mg/m³]	-	1.279	1.332	1.540
μ [mm⁻¹]	-	2.961	1.823	4.870
R₁^a [I > 2.0 σ(I)]	-	0.0425	0.0341	0.0385
wR₂^b (all data)	-	0.0899	0.0782	0.0777
GOF^c	-	1.055	1.184	1.101
CCDC		1471670	1471672	1471667

^a For **5a**, the unit cell only was determined, which is isotypic.

Table S5. Summary of crystallographic data for compounds **6**, **7a** and **7b**

	6	7a	7b
Formula	C ₂₆ H ₅₈ LaN ₃ O ₂	C ₂₀ H ₄₄ ClN ₂ O ₂ Sc	C ₂₀ H ₄₄ ClLuN ₂ O ₂
Fw [g/mol]	583.66	424.98	554.99
T [K]	150(2)	173(2)	173(2)
cryst. system	orthorhombic	monoclinic	monoclinic
space group	Cmc21	P21/c	P21/c
a [Å]	13.323(7)	9.81200(10)	9.9748(2)
b [Å]	15.083(8)	24.1902(3)	24.2613(6)
c [Å]	16.509(9)	12.4810(2)	12.6126(2)
β [°]	90	126.5930(10)	126.4190(10)
Volume [Å³]	3318(3)	2378.50(5)	2456.15(9)
Z	4	4	4
ρ_{calcd} [mg/m³]	1.169	1.187	1.501
μ [mm⁻¹]	1.309	0.437	4.143
R₁^a [I > 2.0 σ(I)]	0.0455	0.0272	0.0210
wR₂^b (all data)	0.1213	0.0272	0.0406
GOF^c	1.090	1.023	1.034
CCDC	1471666	1471665	1471673

Table S6. Summary of crystallographic data for compounds **8**, **9**, and **10**

	8	9	10
Formula	C ₂₄ H ₅₆ LiN ₄ Y	C ₄₆ H ₁₀₂ Cl ₁₀ Li ₂ N ₄ O ₄ Sc ₄	C ₄₀ H ₈₈ Cl ₈ N ₄ O ₄ Sc ₄
Fw [g/mol]	496.58	1323.53	1152.58
T [K]	100(2)	100(2)	100(2)
cryst. system	monoclinic	monoclinic	monoclinic
space group	P21/c	P21/c	P 21/n
a [Å]	17.303(10)	17.7751(14)	11.5846(4)
b [Å]	10.781(6)	8.6911(7)	18.8814(5)
c [Å]	18.467(8)	23.4303(17)	13.1895(4)
β [°]	121.21(4)	111.246(2)	95.116(2)
Volume [Å³]	2946(3)	3373.6(5)	2873.49(15)
Z	4	2	2
ρ_{calcd} [mg/m³]	1.119	1.303	1.332
μ [mm⁻¹]	1.119	0.820	0.862
R₁^a [I > 2.0 σ(I)]	0.0241	0.0548	0.0318
wR₂^b (all data)	0.0569	0.1233	0.0692
GOF^c	1.010	0.998	1.028
CCDC	1471669	1471668	1471675

NMR spectroscopic data

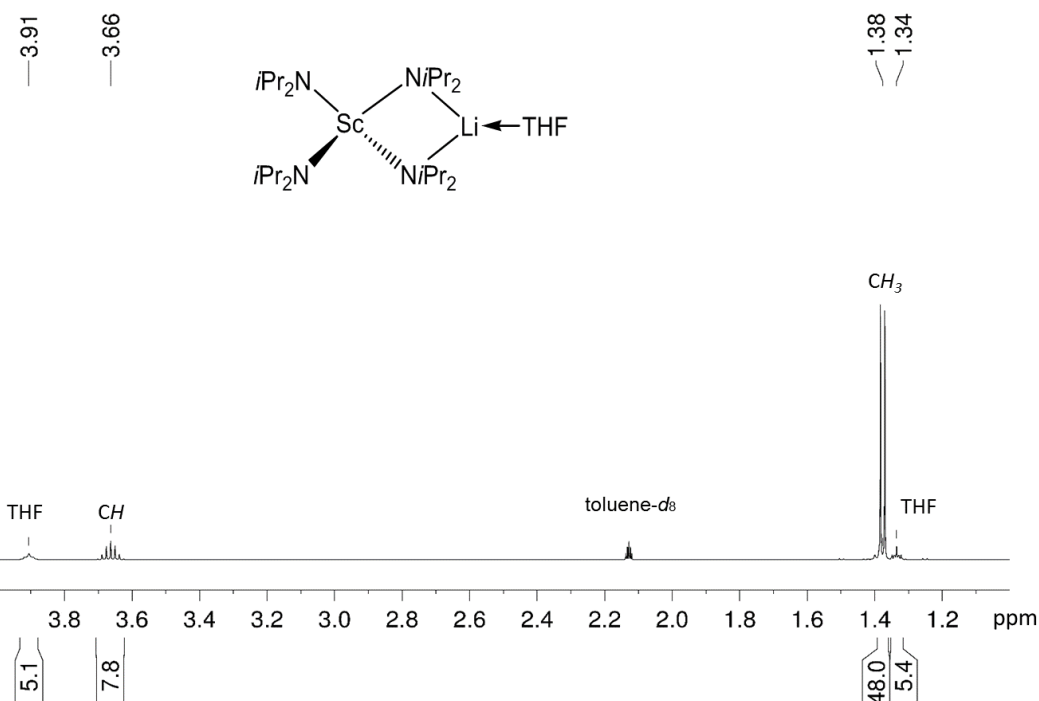


Figure S13. ^1H NMR spectrum (500 MHz) of $\text{LiSc}(\text{NiPr}_2)_4(\text{THF})$ (**1a**) in toluene- d_8 at 26 °C.

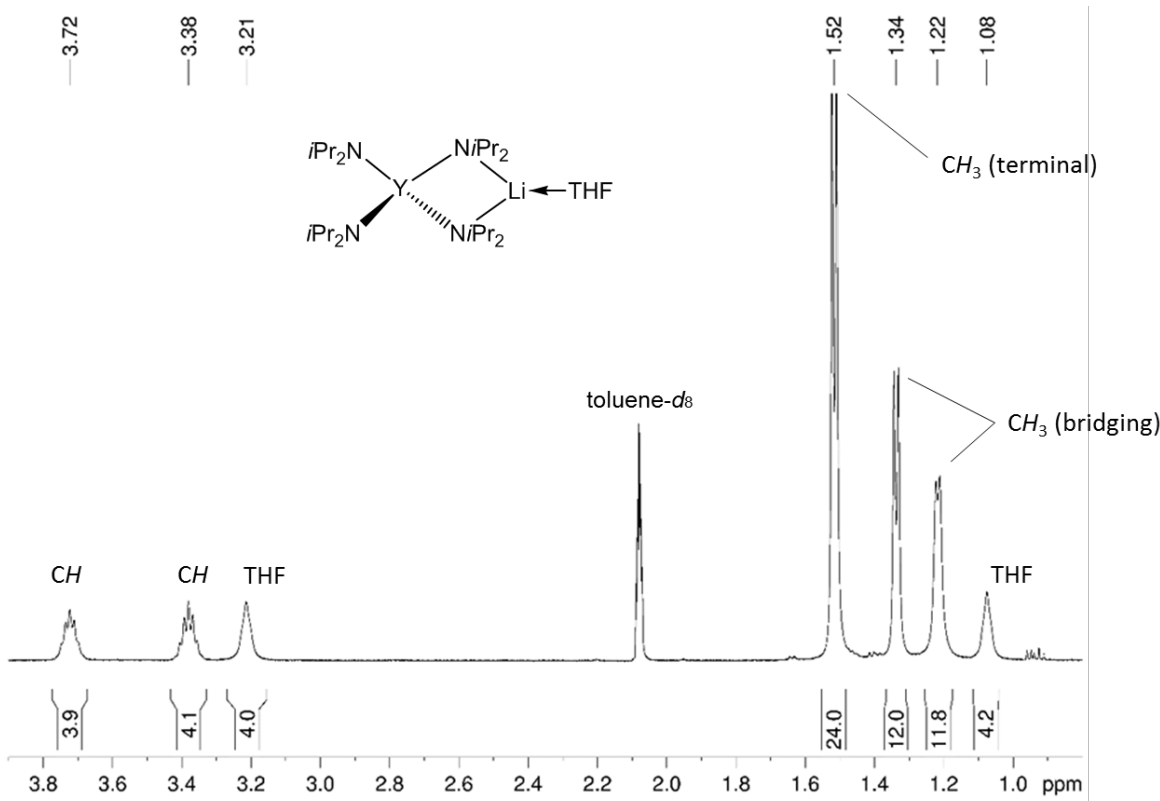


Figure S14. ^1H NMR spectrum (500 MHz) of $\text{LiY}(\text{NiPr}_2)_4(\text{THF})$ (**1b**) in toluene- d_8 at -33 °C.

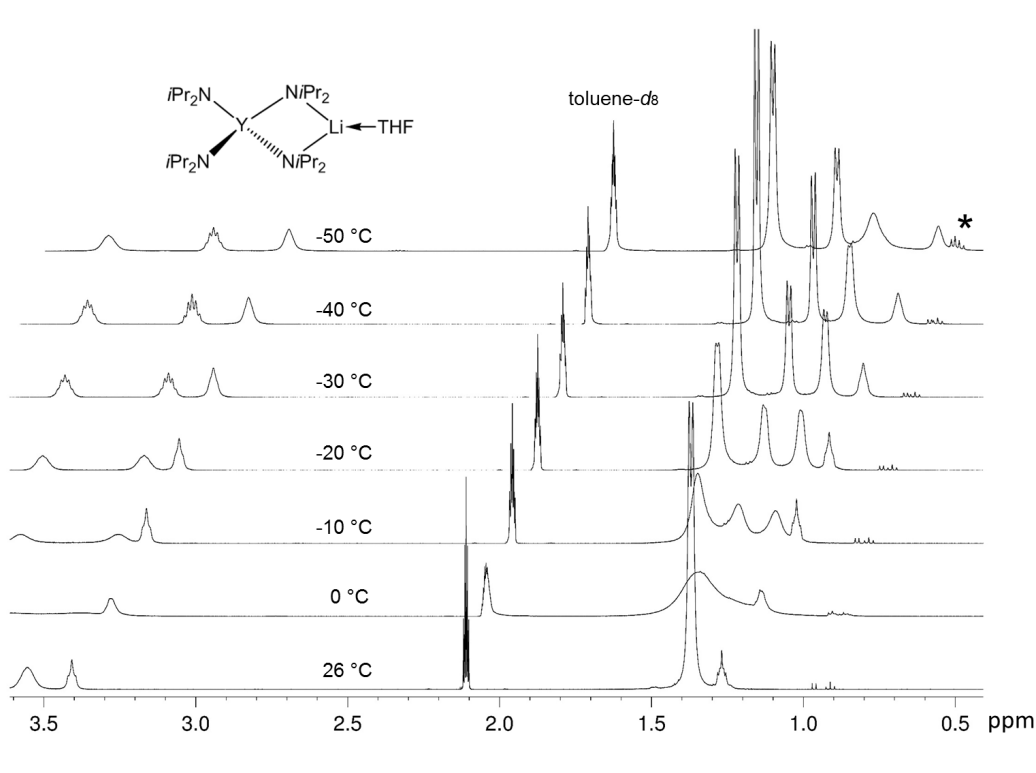


Figure S15. VT ^1H NMR spectra (500 MHz) of $\text{LiY}(\text{NiPr}_2)_4(\text{THF})$ (**1b**) in $\text{toluene}-d_8$; * HNiPr .

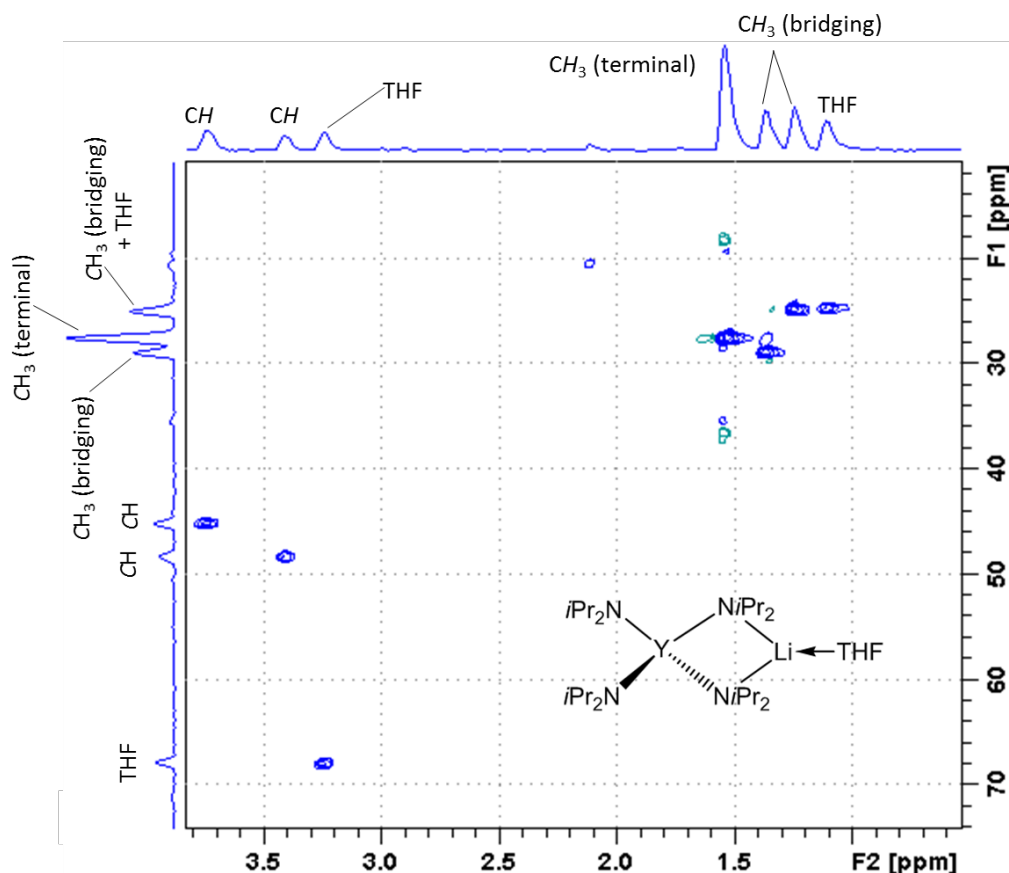


Figure S16. ^1H - ^{13}C HSQC NMR spectrum (500/126 MHz) of $\text{LiY}(\text{NiPr}_2)_4(\text{THF})$ (**1b**) in $\text{toluene}-d_8$ at -30°C .

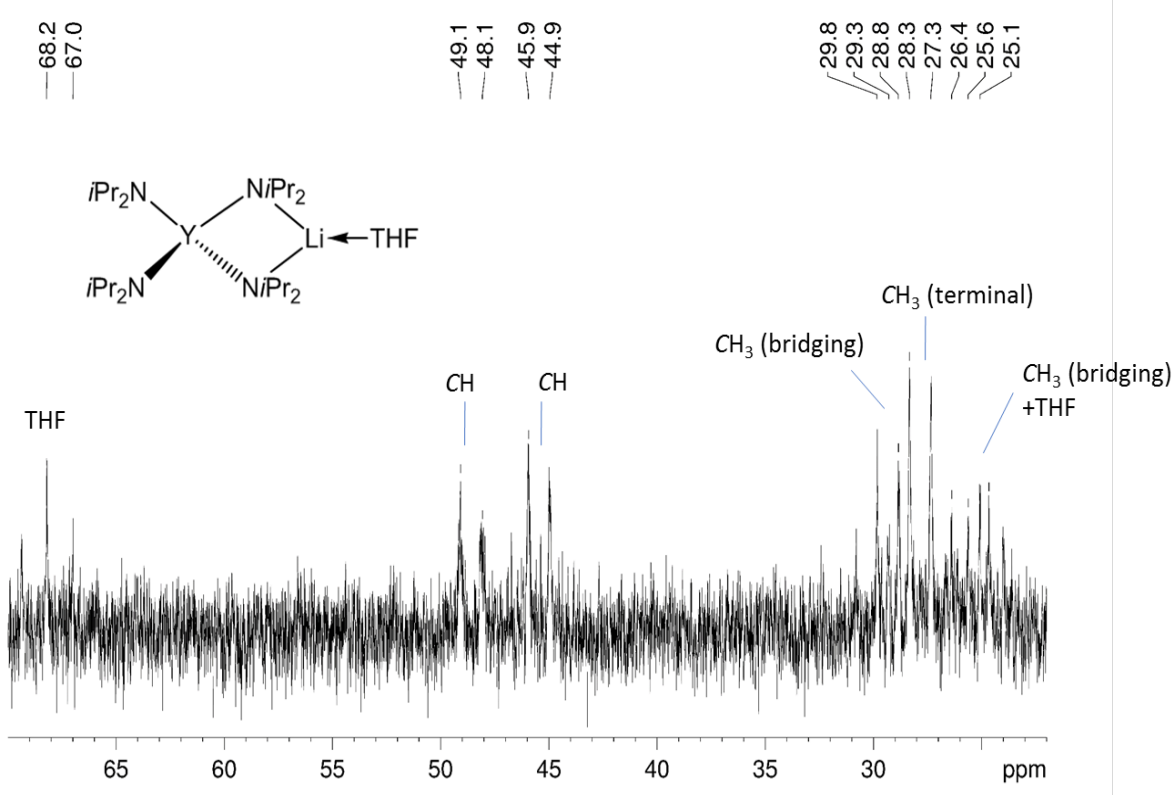


Figure S17. ^{13}C -coupled ^1H NMR spectrum (126 MHz) of $\text{LiY}(\text{NiPr}_2)_4(\text{THF})$ (**1b**) in toluene- d_8 at -35°C .

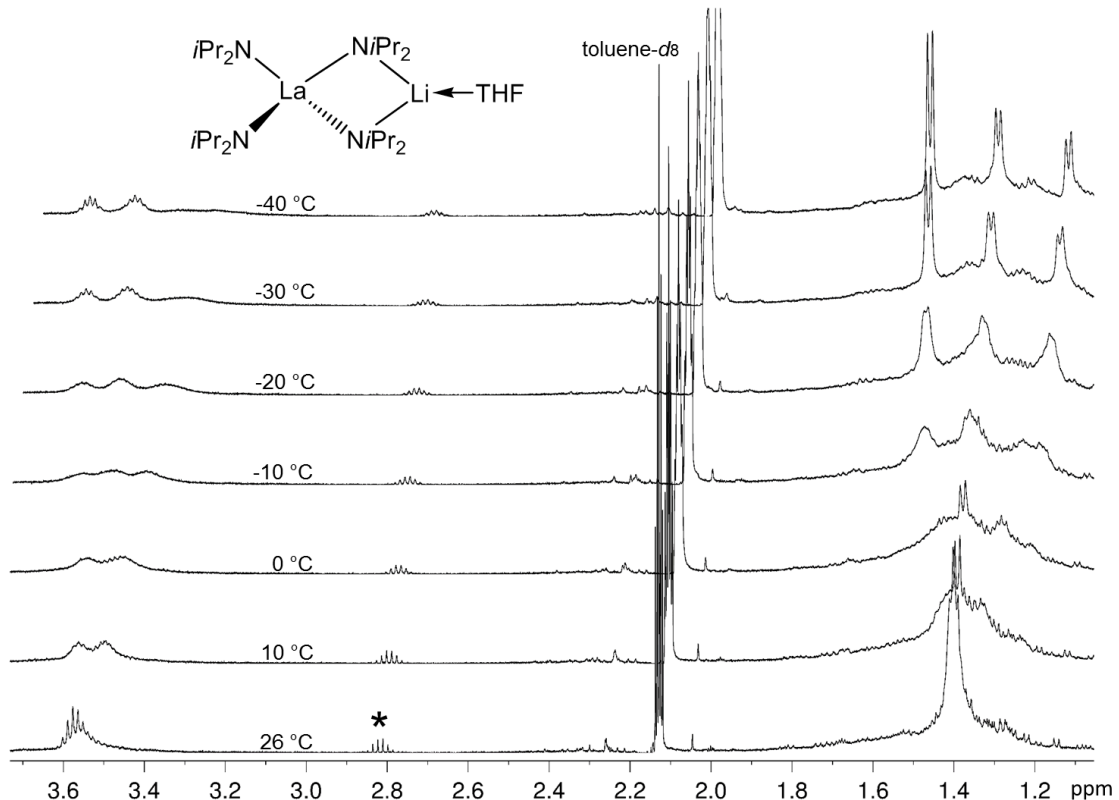


Figure S18. VT ^1H NMR spectra (500 MHz) of $\text{LiLa}(\text{NiPr}_2)_4(\text{THF})$ (**1c**) in toluene- d_8 ; *released HNiPr_2 and residual *n*-hexane.

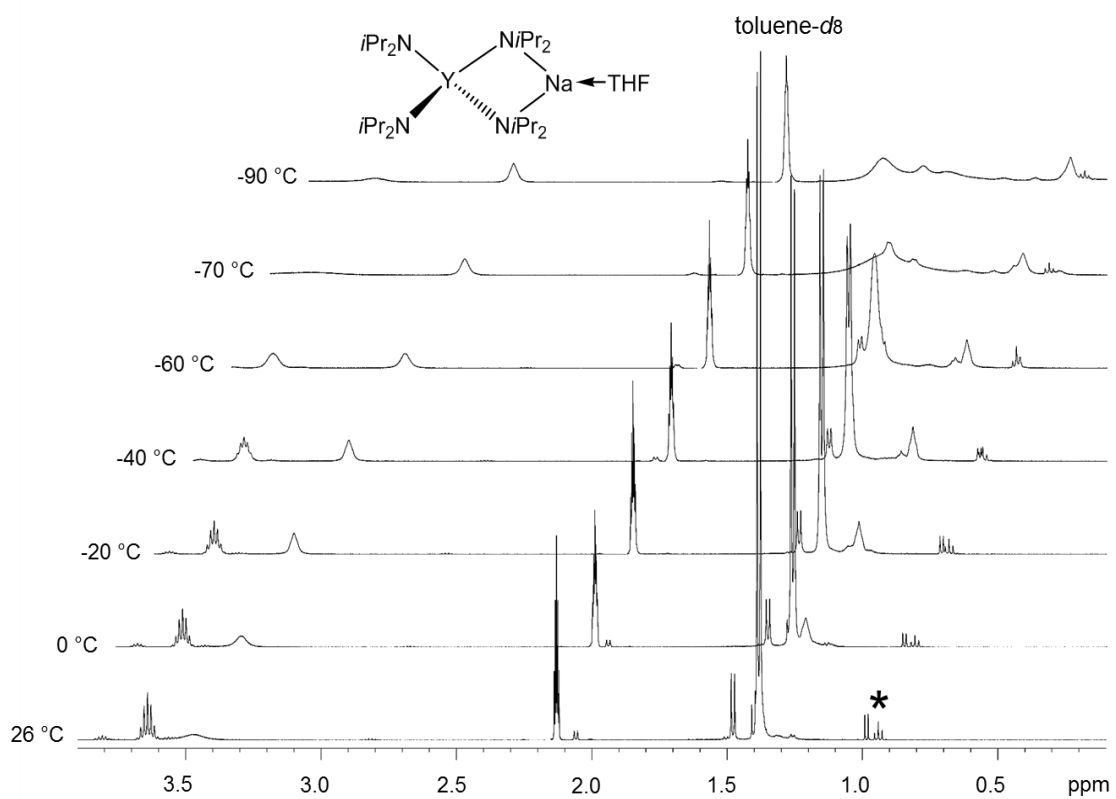


Figure S19. VT ^1H NMR spectra (500 MHz) of $\text{NaY}(\text{NiPr}_2)_4(\text{THF})$ (**2b**) in toluene- d_8 ; *released HNiPr_2 and residual n -hexane.

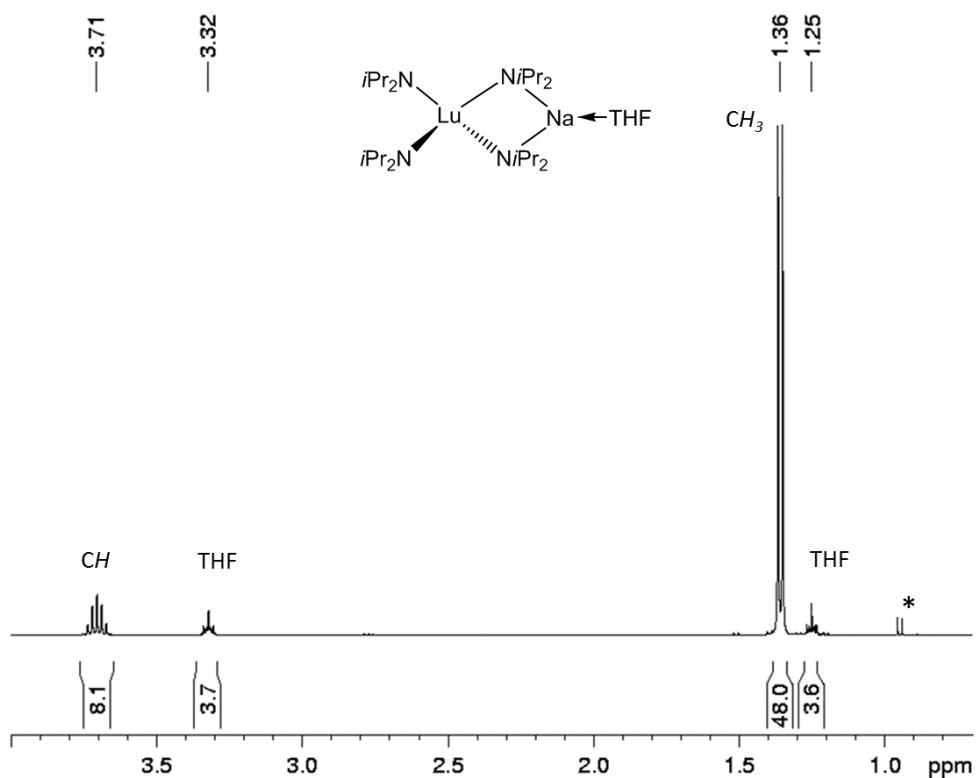


Figure S20. ^1H NMR spectrum (400 MHz) of $\text{NaLu}(\text{NiPr}_2)_4(\text{THF})$ (**2d**) in C_6D_6 at 26°C ; *released HNiPr_2 .

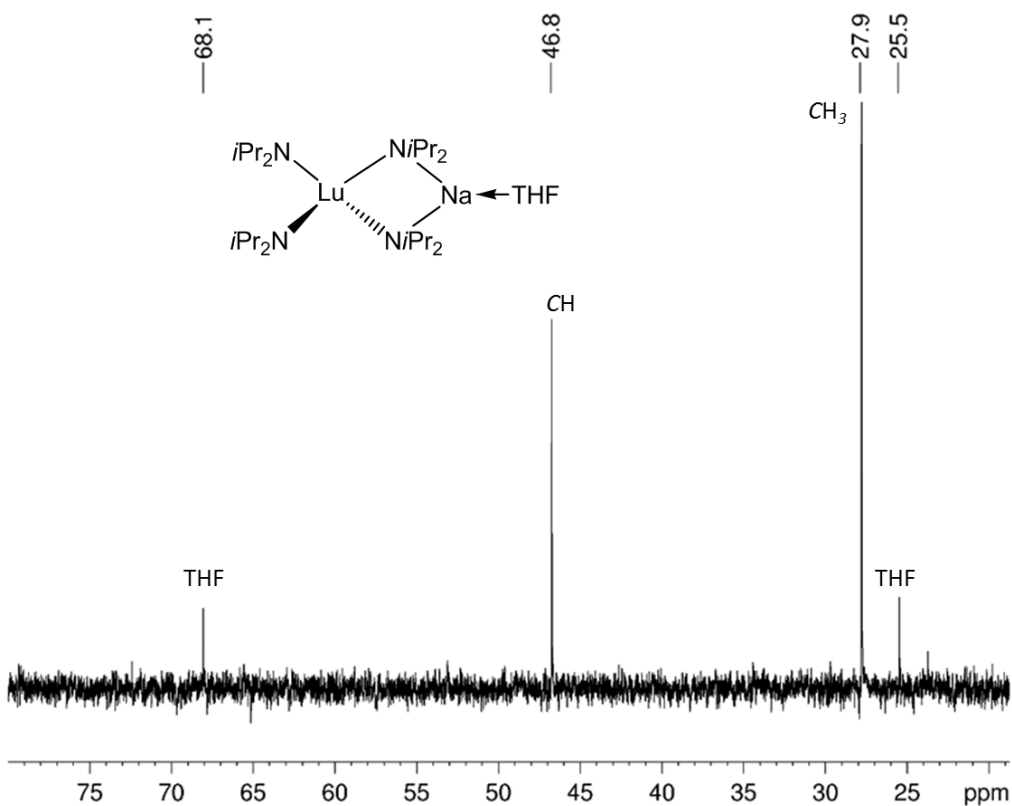


Figure S21. ^{13}C NMR spectrum (101 MHz) of $\text{NaLu}(\text{NiPr}_2)_4(\text{THF})$ (**2d**) in C_6D_6 at 26 °C.

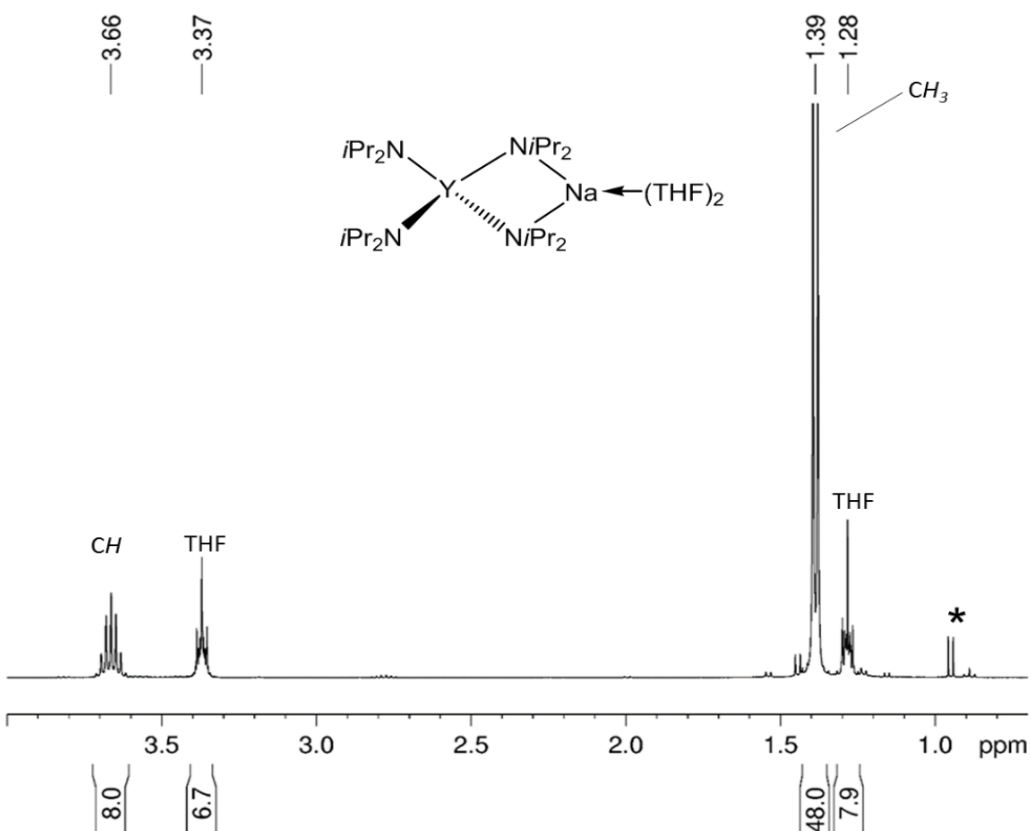


Figure S22. ^1H NMR spectrum (400 MHz) of $\text{NaY}(\text{NiPr}_2)_4(\text{THF})_2$ (**3b**) in C_6D_6 at 26 °C; *released HNiPr_2 .

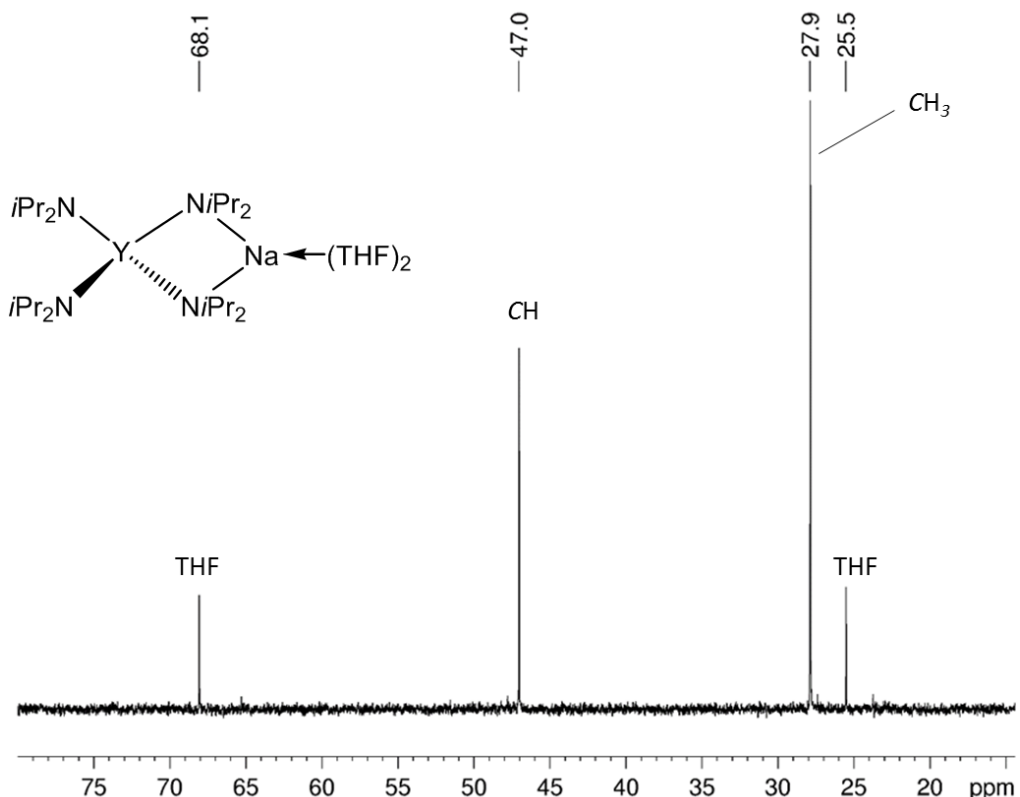


Figure S23. ^{13}C NMR spectrum (101 MHz) of $\text{NaY}(\text{NiPr}_2)_4(\text{THF})_2$ (**3b**) in C_6D_6 at 26°C .

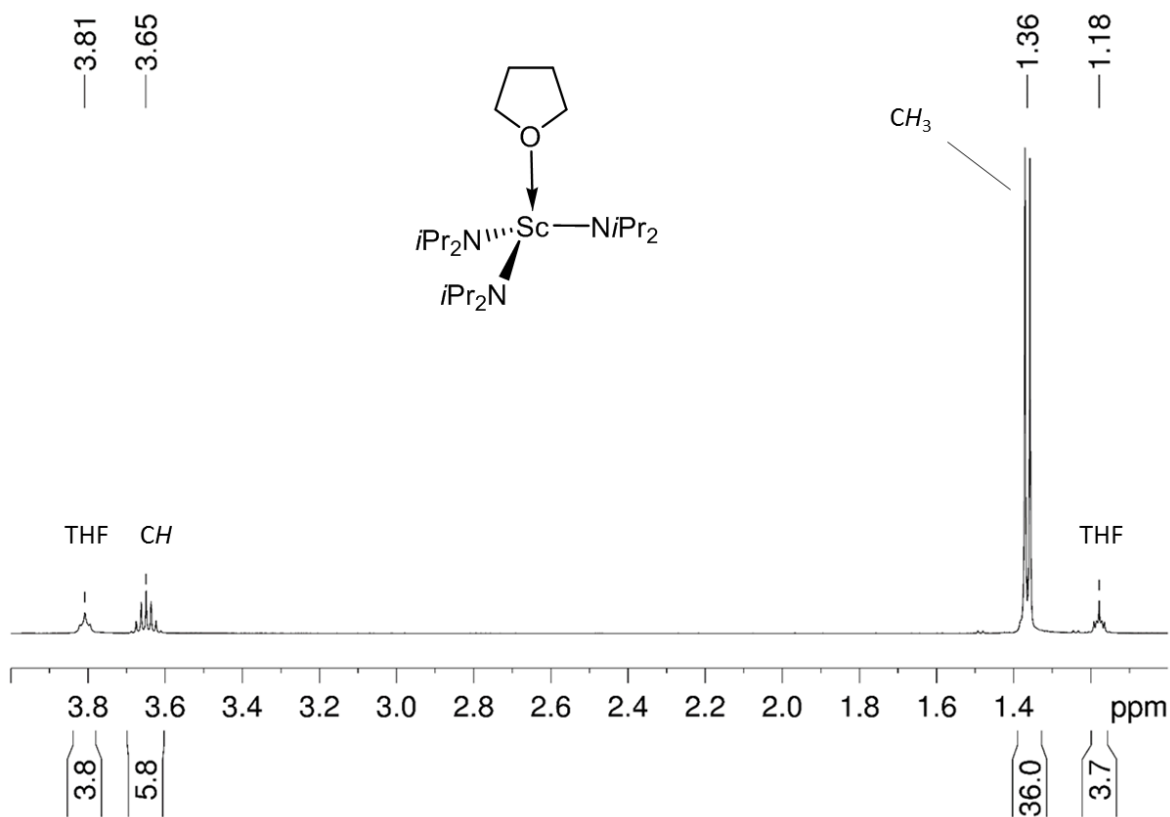


Figure S24. ^1H NMR spectrum (500 MHz) of $\text{Sc}(\text{NiPr}_2)_3(\text{THF})$ (**4a**) in C_6D_6 at 26°C .

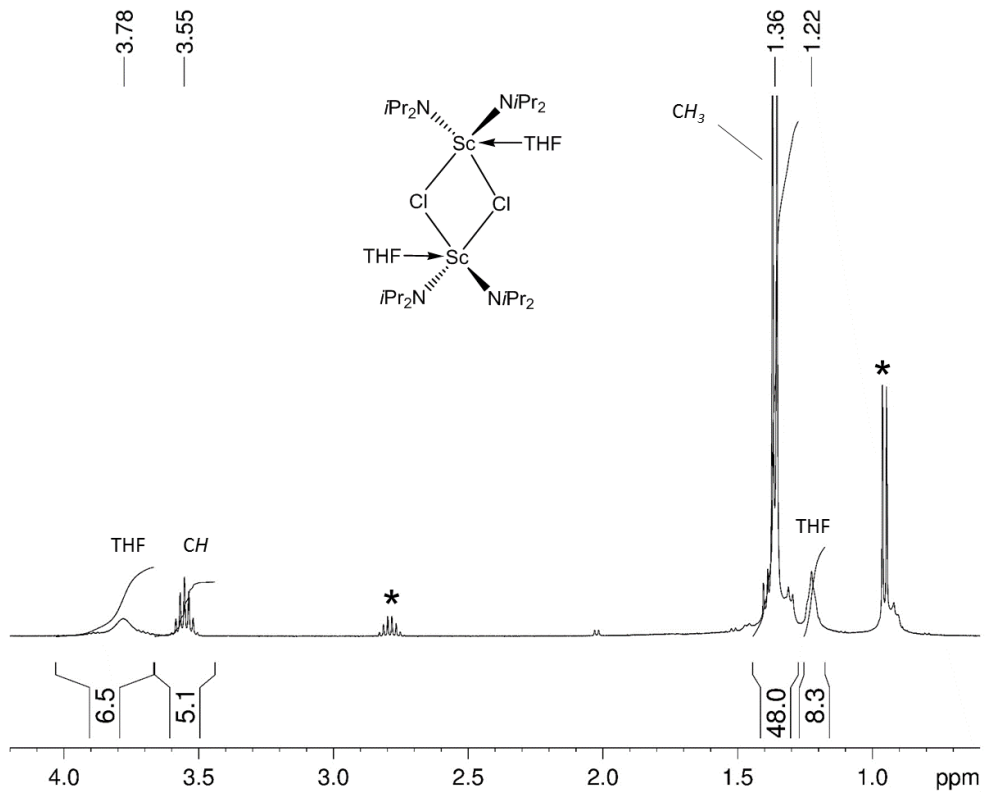


Figure S25. ^1H NMR spectrum (400 MHz) of $\text{Sc}[(\text{NiPr}_2)_2(\text{THF})(\mu\text{-Cl})]_2$ (**5a**) in C_6D_6 at 26 °C. Integral mismatch because of significant decomposition as seen by released HNiPr_2 (*).

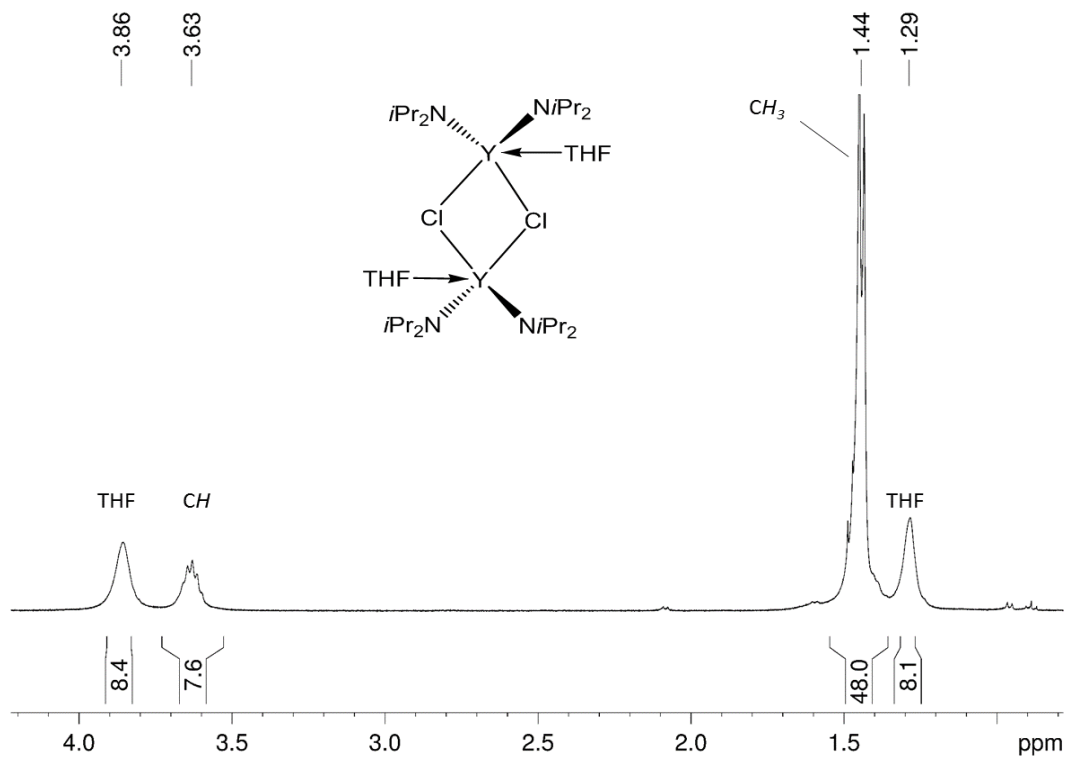


Figure S26. ^1H NMR spectrum (400 MHz) of $\text{Y}[(\text{NiPr}_2)_2(\text{THF})(\mu\text{-Cl})]_2$ (**5b**) in C_6D_6 at 26 °C.

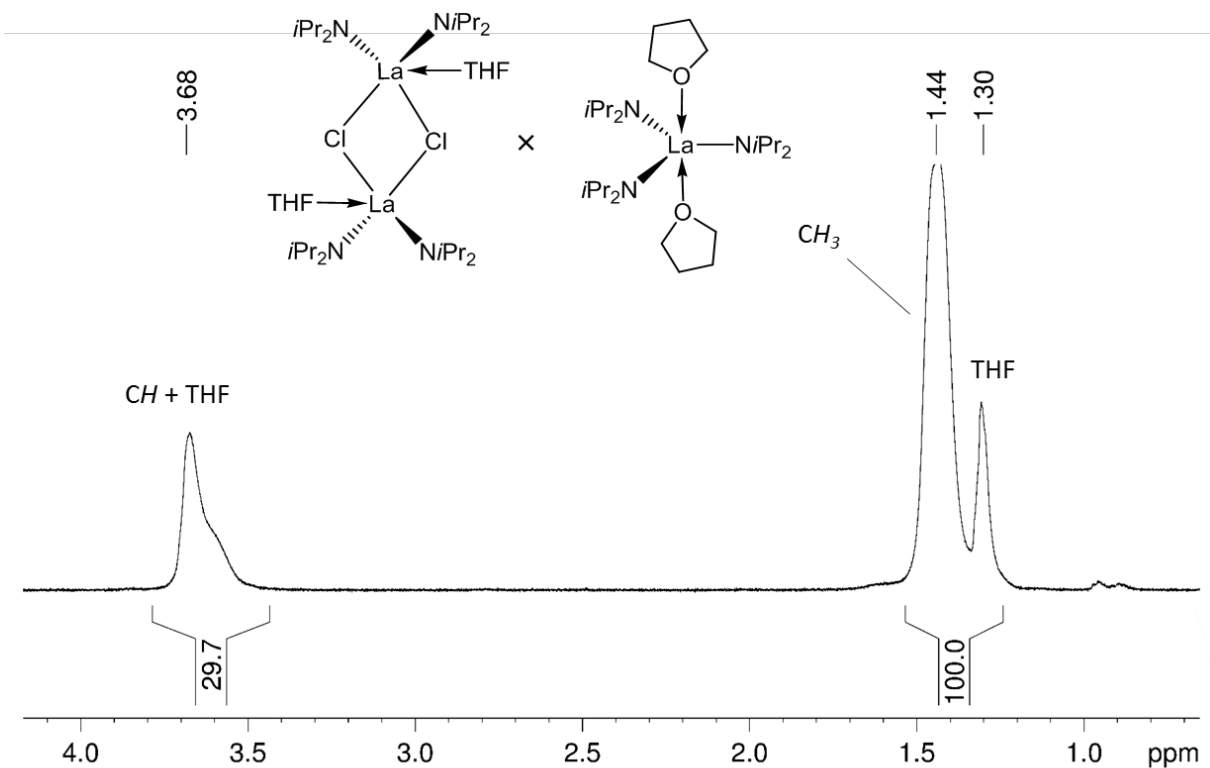


Figure S27. ^1H NMR spectrum (400 MHz) of $[\text{La}(\text{NiPr}_2)_2(\text{THF})(\mu\text{-Cl})]_2 \times \text{La}(\text{NiPr}_2)_3(\text{THF})_2$ (**5c'**) in C_6D_6 at 26 °C.

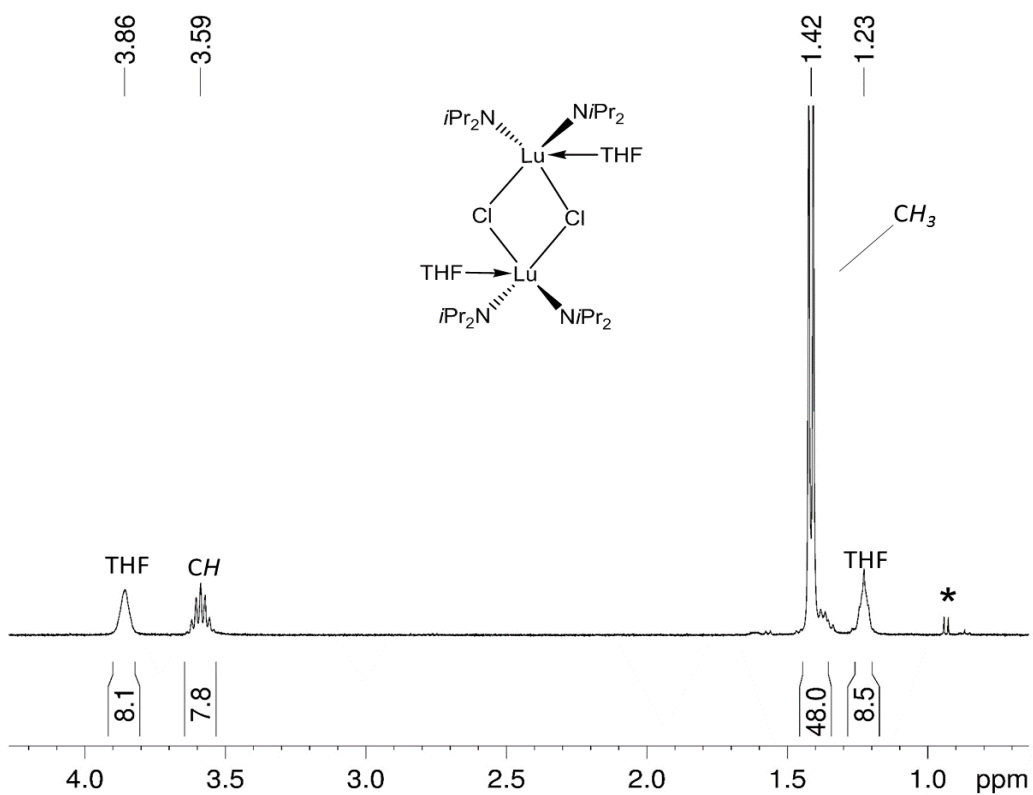


Figure S28. ^1H NMR spectrum (400 MHz) of $\text{Lu}[(\text{NiPr}_2)_2(\text{THF})(\mu\text{-Cl})]_2$ (**5d**) in C_6D_6 at 26 °C.

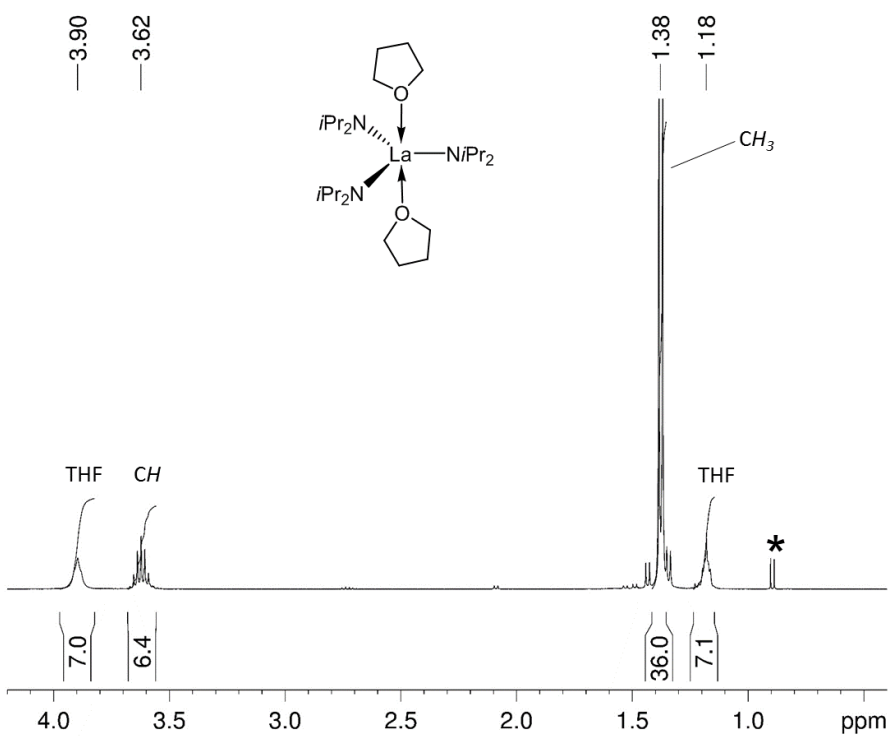


Figure S29. ^1H NMR spectrum (400 MHz) of $\text{La}(\text{NiPr}_2)_3(\text{THF})_2$ (**6**) in C_6D_6 at 26 °C; *released HNiPr_2 .

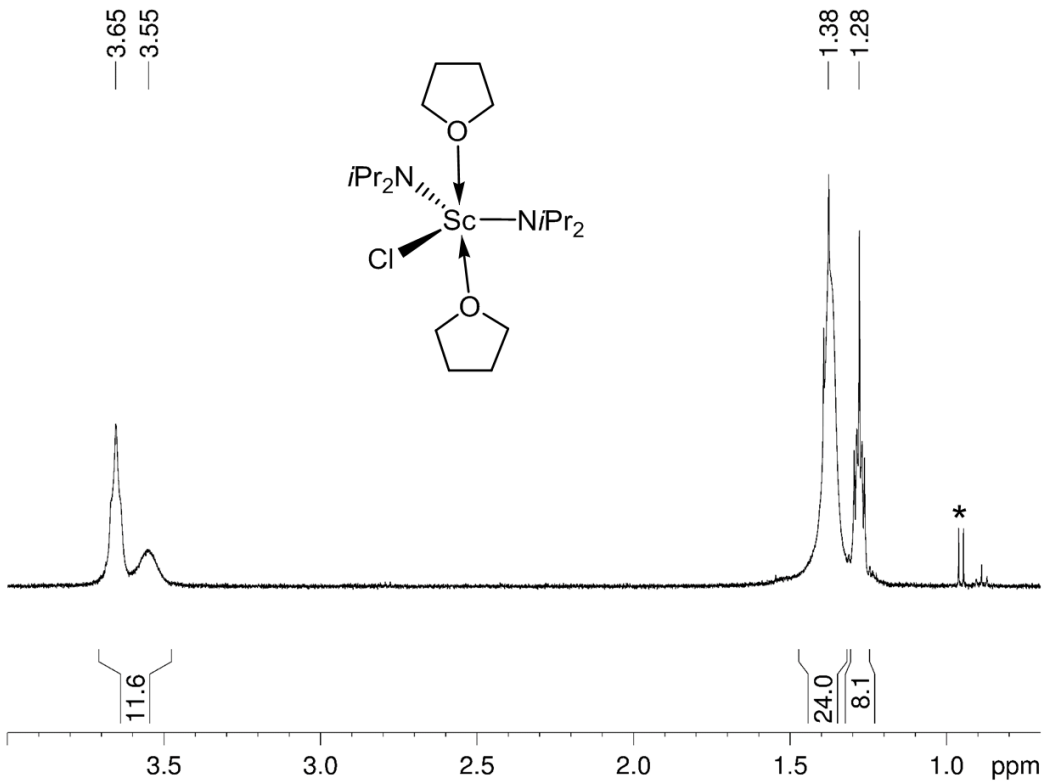


Figure S30. ^1H NMR spectrum (400 MHz) of $\text{Sc}(\text{NiPr}_2)_2\text{Cl}(\text{THF})_2$ (**7a**) in C_6D_6 at 26 °C; *released HNiPr_2 .

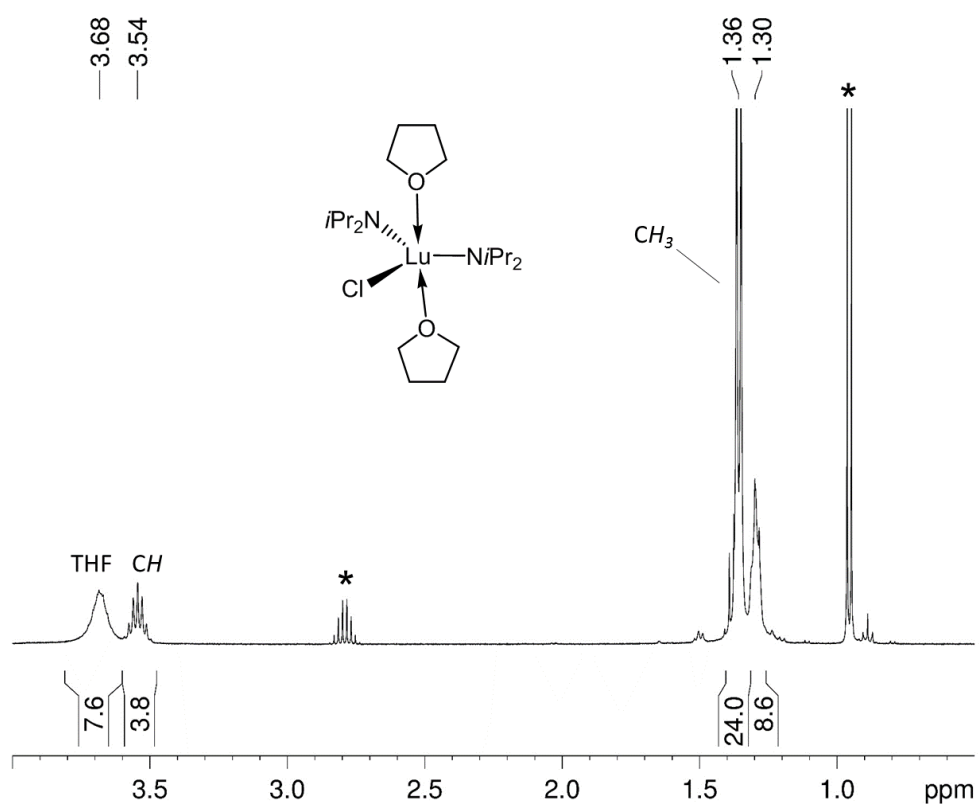


Figure S31. ^1H NMR spectrum (400 MHz) of $\text{Lu}(\text{NiPr}_2)_2\text{Cl}(\text{THF})_2$ (**7b**) in C_6D_6 at 26 °C, *released HNiPr_2 .

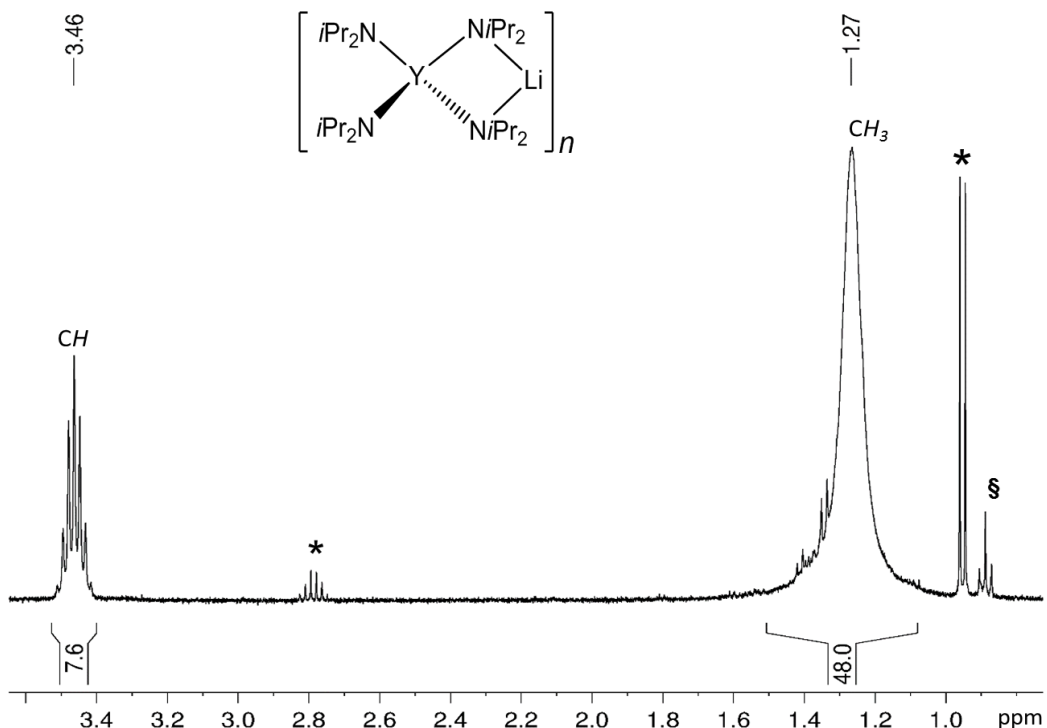


Figure S32. ^1H NMR spectrum (500 MHz) of $[\text{LiY}(\text{NiPr}_2)_4]_n$ (**8**) in C_6D_6 at 26 °C, *released HNiPr_2 and § residual *n*-hexane.

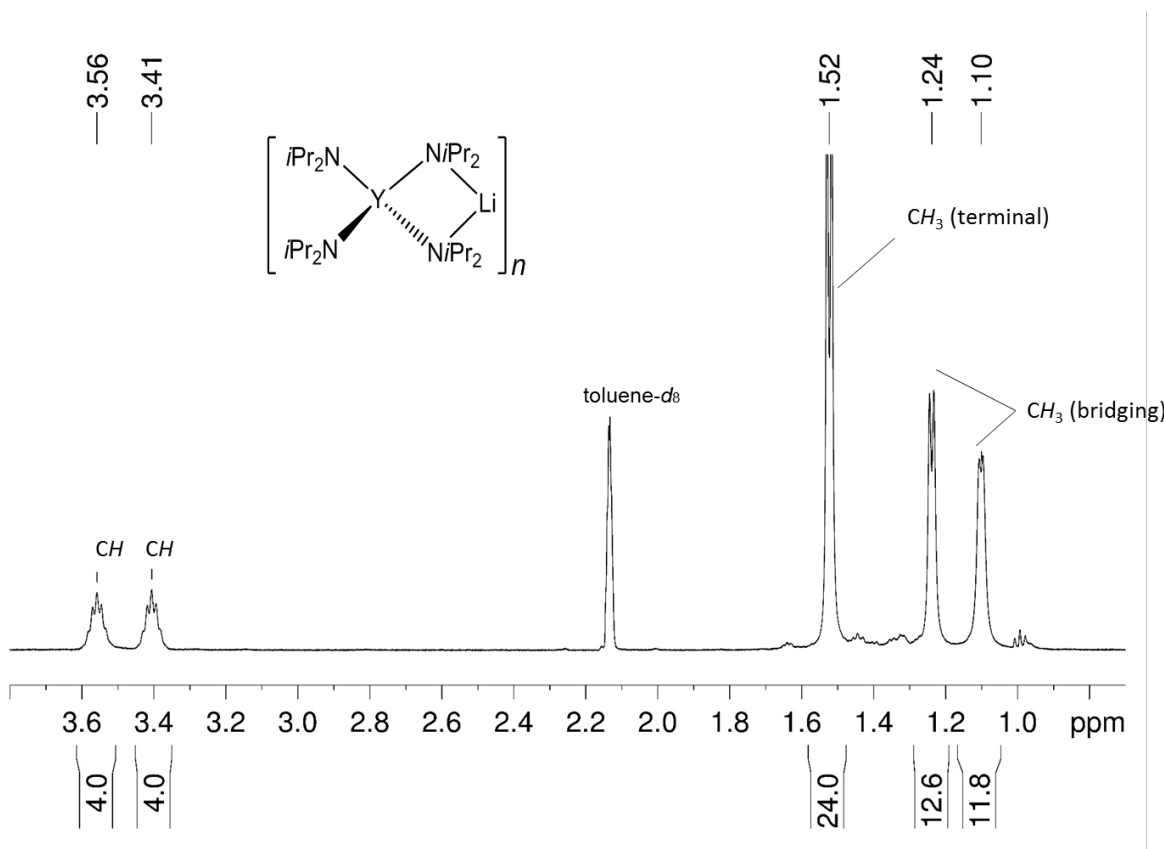


Figure S33. ^1H NMR spectrum (500 MHz) of $[\text{LiY}(\text{NiPr}_2)_4]_n$ (**8**) in C_6D_6 at -50°C .

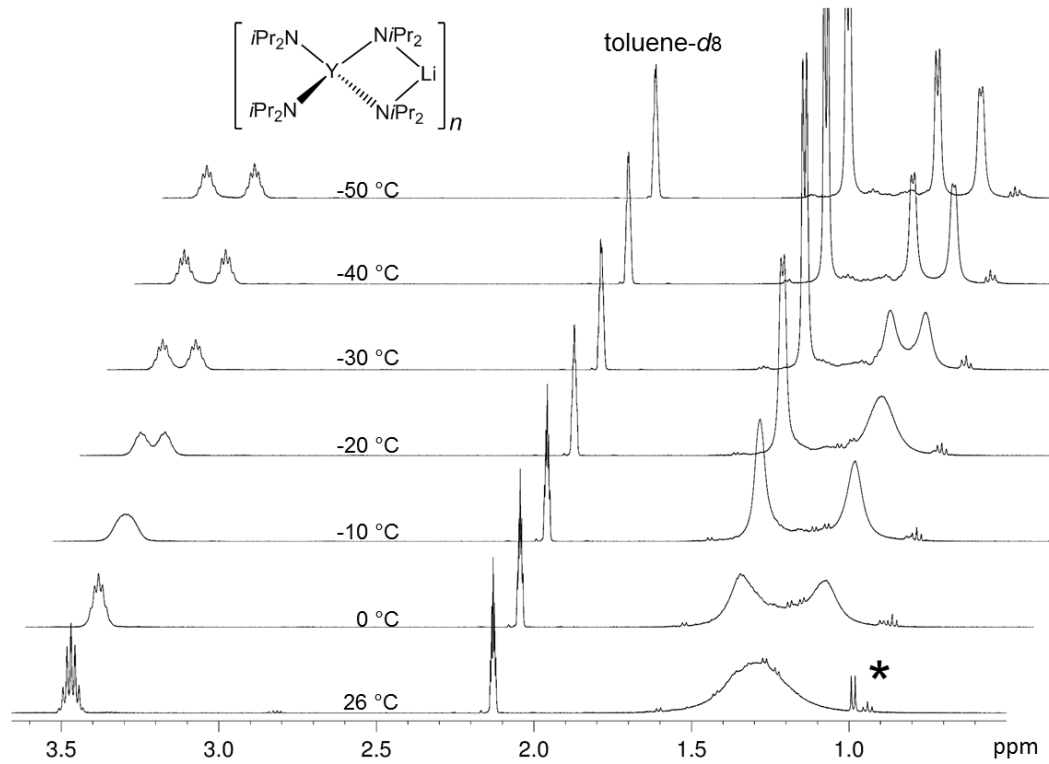


Figure S34. VT ^1H NMR spectra (500 MHz) of $[\text{LiY}(\text{NiPr}_2)_4]_n$ (**8**) in toluene- d_8 ; * HNiPr_2 and residual *n*-hexane.

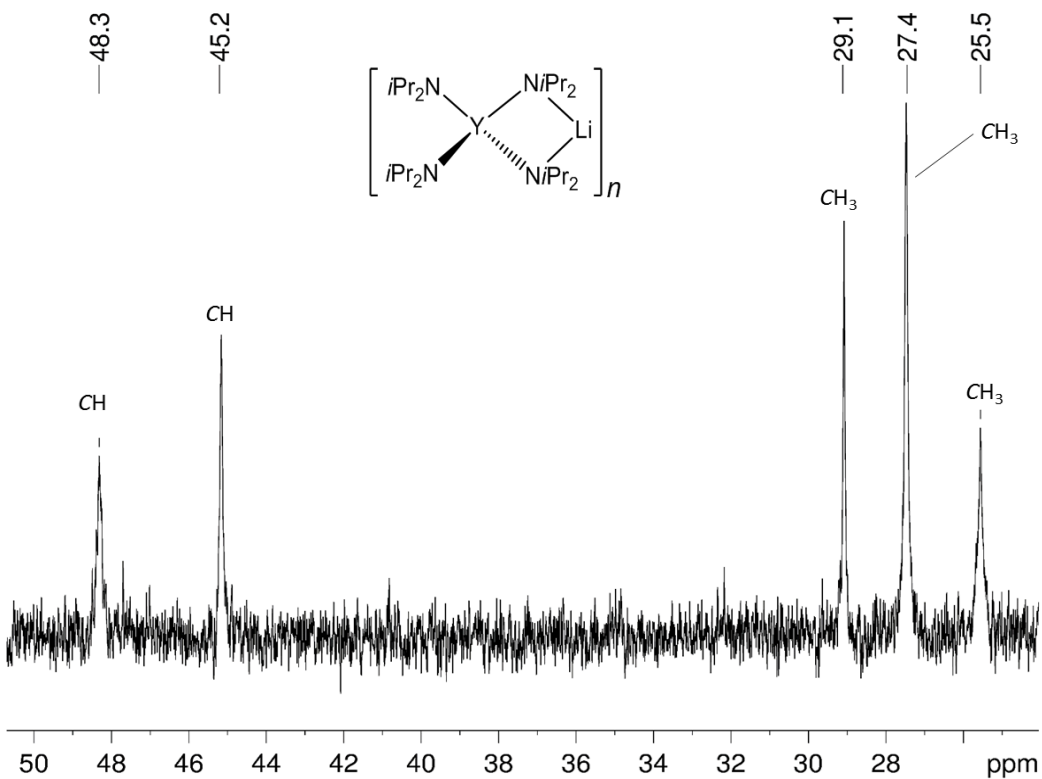


Figure S35. ^{13}C NMR spectrum (500 MHz) of $[\text{LiY}(\text{NiPr}_2)_4]_n$ (8) in toluene- d_8 at -50 °C.

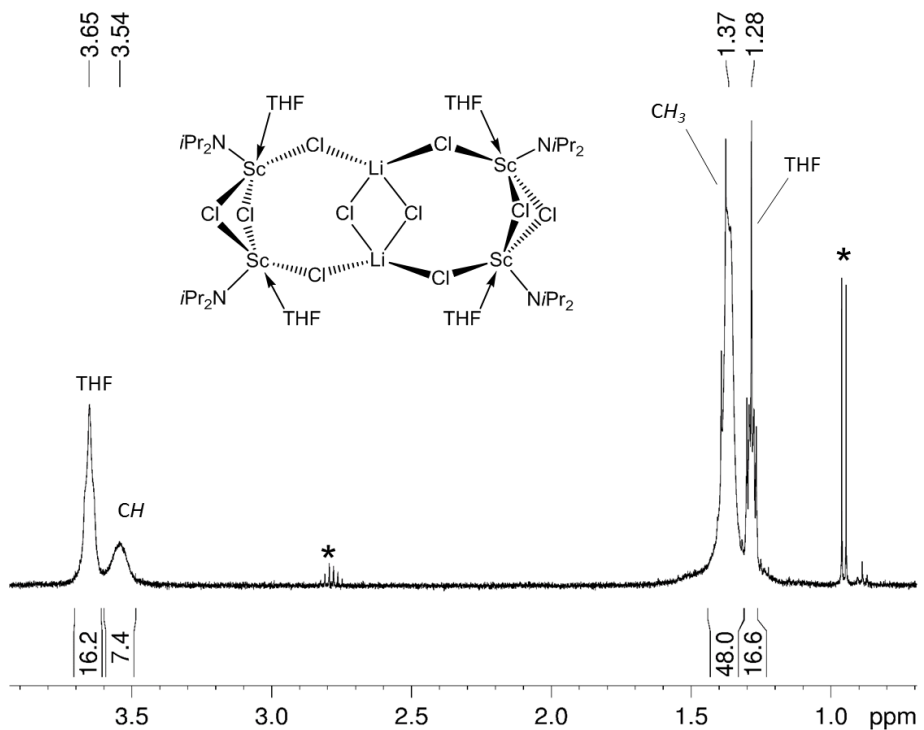


Figure S36. ^1H NMR spectrum (400 MHz) of $\{[\text{Sc}(\text{NiPr}_2)\text{Cl}_2(\text{THF})]_2(\text{LiCl})\}_2$ (9) in C_6D_6 at 26 °C; *released HNiPr_2 .

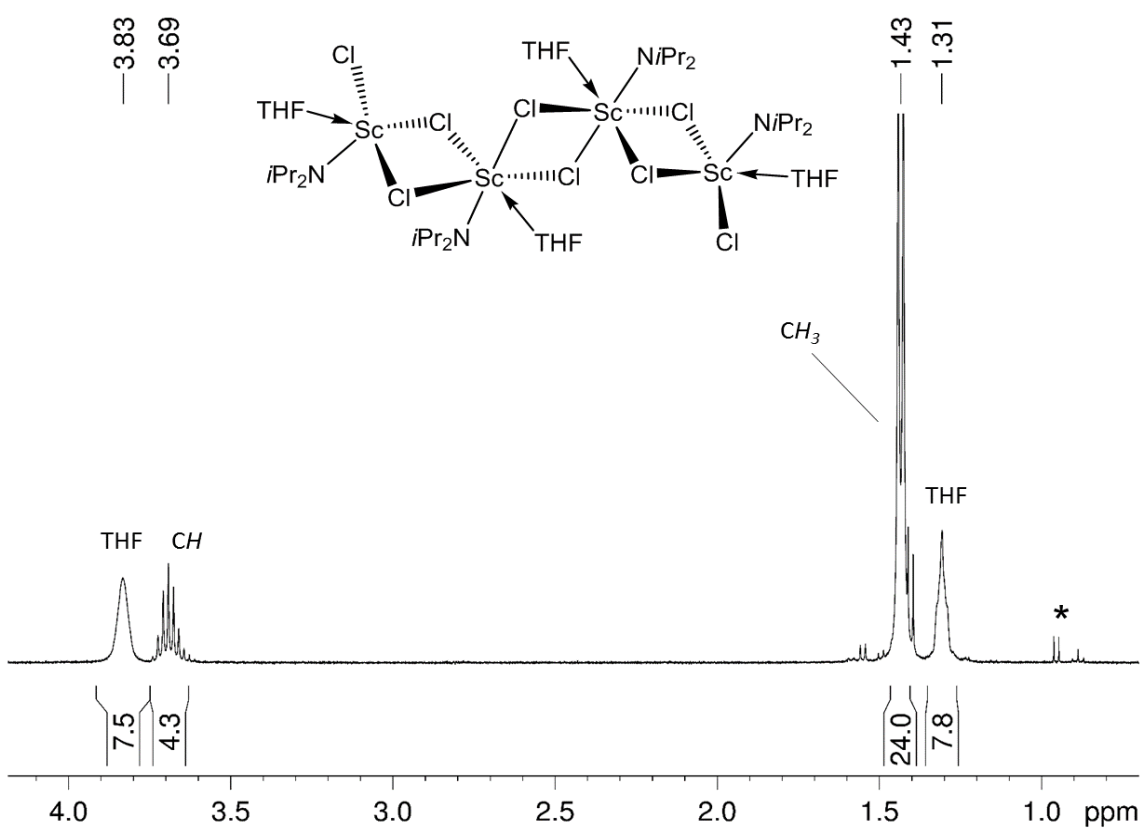


Figure S37. 1H NMR spectrum (400 MHz) of $[Sc(NiPr_2)Cl_2(THF)]_4$ (**10**) in C_6D_6 at 26 °C;
*released $HNiPr_2$.

DFT Calculations

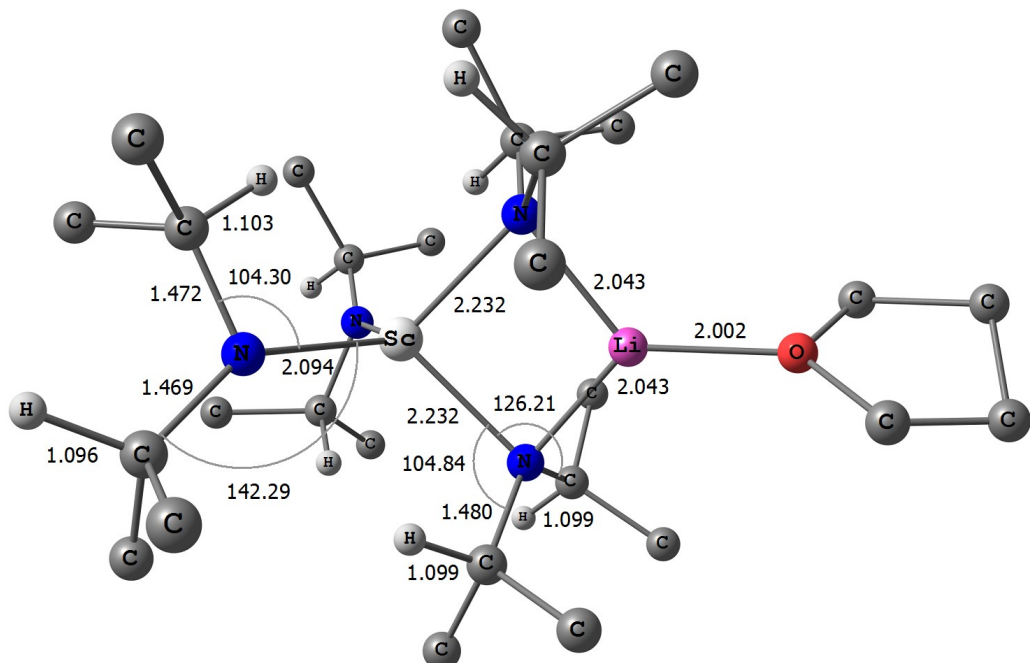


Figure S38. DFT-optimised geometry ([B3LYP/def2-TZVP] level of theory) and selected geometrical parameters of $\text{LiSc}(\text{NiPr}_2)_4(\text{THF})$ (**1a'**). All hydrogen atoms are omitted for clarity, except for the ones attached to the β -C atoms.

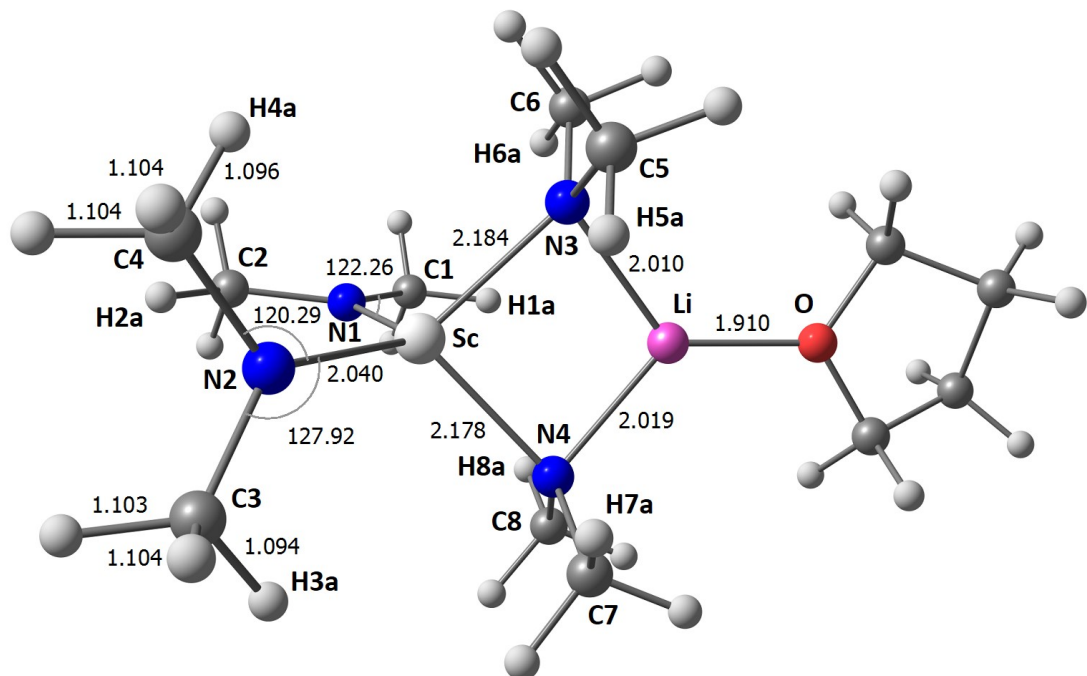


Figure S39. DFT-optimised geometry ([B3LYP/def2-TZVP] level of theory) and selected geometrical parameters of $\text{LiSc}(\text{NMe}_2)_4(\text{THF})$ (**1a''**).

Table S7. Selected geometrical parameters for the DFT model system LiSc(NMe₂)₄(THF) **1a''** (distances in Å, angles in °).

Sc–N1	2.042	C5–H5a	1.094
Sc–N2	2.040	C6–H6a	1.092
Sc–N3	2.184	H1a···Sc	3.017
Sc–N4	2.178	H2a···Sc	3.115
N1–C1	1.447	H3a···Sc	3.145
N1–C2	1.447	H4a···Sc	2.962
N2–C3	1.443	H5a···Sc	3.115
N2–C4	1.446	H6a···Sc	3.216
N3–C5	1.459	Sc–N1–C1	122.26
N3–C6	1.457	Sc–N1–C2	126.75
N4–C7	1.459	Sc–N2–C3	127.92
N4–C8	1.456	Sc–N2–C4	120.29
C1–H1a	1.097	Sc–N3–C5	117.04
C2–H2a	1.092	Sc–N3–C6	120.59
C3–H3a	1.094	Sc–N4–C7	116.88
C4–H4a	1.096	Sc–N4–C8	121.60

Table S8. Cartesian coordinates of the DFT-optimised model system LiSc(NiPr₂)₄(THF) **1a'** (B3LYP/def2-TZVP level of theory).

6	3.219215000	-2.638815000	-1.659491000
6	1.656762000	-2.002146000	-3.533183000
6	2.658889000	-1.476019000	-2.489142000
6	4.245417000	1.027380000	-1.727508000
6	2.424098000	1.431083000	-3.406924000
6	2.729965000	0.924338000	-1.983340000
6	4.245549000	-1.027338000	1.727406000
6	0.259703000	-3.858664000	0.427006000
6	2.730100000	-0.924388000	1.983281000
6	-0.399536000	-2.657074000	-0.272036000
6	-1.606635000	-3.139262000	-1.102433000
6	-1.261313000	0.472615000	-2.746149000
6	3.219169000	2.638801000	1.659452000
6	2.424309000	-1.431188000	3.406863000
6	2.659006000	1.475947000	2.489131000
6	-1.101460000	1.773680000	-1.956811000
6	0.260092000	3.858556000	-0.427158000
6	-0.399337000	2.657117000	0.271963000
6	-2.418900000	2.567302000	-2.075490000
6	-1.101515000	-1.773739000	1.956819000
6	1.656991000	2.001987000	3.533325000
6	-2.418969000	-2.567342000	2.075467000
6	-1.261327000	-0.472721000	2.746240000
6	-4.773738000	-0.794369000	-0.881953000
6	-1.606387000	3.139544000	1.102296000
6	-6.185590000	-0.696819000	-0.317944000
6	-4.773660000	0.794551000	0.882054000
6	-6.185557000	0.697013000	0.318153000
1	3.634971000	-3.415654000	-2.307820000
1	2.120534000	-2.766287000	-4.164291000
1	3.508491000	-1.097880000	-3.068739000
1	4.810198000	0.373826000	-2.395748000

1	2.919066000	0.809973000	-4.157122000
1	4.010025000	-2.293350000	-0.993961000
1	1.307519000	-1.197597000	-4.180799000
1	4.596217000	2.048402000	-1.900243000
1	2.446669000	-3.104826000	-1.046678000
1	0.781893000	-2.453205000	-3.060486000
1	2.788129000	2.453500000	-3.541393000
1	4.483342000	0.753641000	-0.702169000
1	4.483434000	-0.753562000	0.702067000
1	4.596414000	-2.048343000	1.900110000
1	1.354976000	1.419005000	-3.611982000
1	4.810309000	-0.373764000	2.395645000
1	0.574817000	-4.593097000	-0.316962000
1	2.268653000	1.656177000	-1.299371000
1	0.326730000	-2.324516000	-1.026555000
1	2.268800000	-1.656226000	1.299304000
1	4.009912000	2.293399000	0.993807000
1	-1.297903000	-3.909753000	-1.814918000
1	1.141493000	-3.562128000	0.995630000
1	-0.359398000	-0.135519000	-2.698586000
1	2.788391000	-2.453592000	3.541288000
1	-1.471746000	0.684068000	-3.796643000
1	-0.422773000	-4.364156000	1.111281000
1	-0.341019000	2.367479000	-2.483633000
1	3.508697000	1.097822000	3.068609000
1	-2.030979000	-2.316513000	-1.679295000
1	1.141847000	3.561842000	-0.995746000
1	3.634969000	3.415638000	2.307755000
1	2.919278000	-0.810078000	4.157059000
1	2.446519000	3.104794000	1.046753000
1	-2.393793000	-3.563477000	-0.478710000
1	-2.104311000	-0.121282000	-2.375020000
1	1.355195000	-1.419163000	3.611964000
1	-2.689186000	2.681206000	-3.129110000
1	-0.422295000	4.364101000	-1.111481000
1	-0.341082000	-2.367591000	2.483593000
1	0.326872000	2.324523000	1.026519000
1	0.575308000	4.592994000	0.316762000
1	-2.348218000	-3.566781000	1.651293000
1	-2.348131000	3.566760000	-1.651365000
1	2.120811000	2.766127000	4.164398000
1	1.307877000	1.197397000	4.180959000
1	-0.359404000	0.135401000	2.698695000
1	-3.236223000	2.043791000	-1.572860000
1	0.782037000	2.453021000	3.060764000
1	-4.711348000	-0.371473000	-1.888530000
1	-4.378356000	-1.808942000	-0.899721000
1	-3.236286000	-2.043793000	1.572866000
1	-2.689250000	-2.681294000	3.129083000
1	-2.104322000	0.121211000	2.375164000
1	-1.471742000	-0.684234000	3.796726000
1	-2.393467000	3.563828000	0.478522000
1	-2.030865000	2.316901000	1.679210000
1	-1.297560000	3.910044000	1.814730000
1	-6.945279000	-0.817798000	-1.089445000
1	-4.378258000	1.809117000	0.899758000
1	-6.347388000	-1.464252000	0.441761000
1	-6.347408000	1.464447000	-0.441540000
1	-4.711202000	0.371689000	1.888641000
1	-6.945184000	0.818000000	1.089713000
7	2.134110000	-0.382818000	-1.660252000
7	2.134180000	0.382753000	1.660261000
7	-0.653015000	-1.475680000	0.583429000

7	-0.652948000	1.475685000	-0.583411000
8	-3.942019000	0.000065000	0.000035000
3	-1.940068000	0.000054000	0.000053000
21	0.916762000	-0.000021000	0.000024000

Table S9. Cartesian coordinates of the DFT-optimised model system LiSc(NMe₂)₄(THF) **1a''** (B3LYP/def2-TZVP level of theory).

1	-0.474101000	2.550714000	-1.289558000
1	-1.756901000	3.005980000	-2.413191000
6	-1.541113000	2.797881000	-1.350652000
1	-4.006863000	2.990483000	-0.336174000
1	-4.094255000	2.242403000	-1.934956000
6	-3.763832000	2.071079000	-0.896143000
1	-4.753920000	-0.945818000	1.672741000
1	-0.636414000	2.097227000	2.727625000
6	-3.669316000	-1.085720000	1.821029000
6	0.107960000	1.827821000	1.961224000
1	1.097101000	1.986014000	2.426966000
1	0.021933000	0.714882000	-2.786263000
1	-2.933394000	-2.628080000	-1.057284000
1	-3.554393000	-1.921384000	2.532864000
6	-3.458223000	-2.480600000	-0.108548000
6	0.163068000	-0.366127000	-2.722481000
1	-0.550046000	-2.816446000	-1.991942000
6	0.138383000	-2.286652000	-1.314165000
1	1.174386000	-0.590619000	-3.106401000
6	0.051294000	-0.469613000	2.581642000
1	-3.329075000	-3.405779000	0.480210000
1	1.044833000	-0.434657000	3.064301000
1	-0.114874000	-1.498690000	2.249502000
6	3.940930000	0.548412000	1.091627000
1	1.155214000	-2.605040000	-1.606160000
6	5.371559000	0.101381000	0.818077000
6	3.994922000	-0.602948000	-0.989775000
6	5.382499000	-0.041315000	-0.708237000
1	-1.676626000	3.751716000	-0.811392000
1	-4.376301000	1.264793000	-0.487250000
1	0.008193000	2.553605000	1.151131000
1	-3.298820000	-0.185802000	2.325530000
1	-0.541028000	-0.826934000	-3.433592000
1	-4.534178000	-2.408188000	-0.342581000
1	-0.680574000	-0.271840000	3.381264000
1	-0.047448000	-2.675601000	-0.307852000
1	3.834355000	1.634137000	1.024157000
1	3.551213000	0.215677000	2.053208000
1	6.104007000	0.818023000	1.187722000
1	3.587786000	-0.311130000	-1.957329000
1	5.568936000	-0.861736000	1.293276000
1	5.503067000	0.934869000	-1.182492000
1	3.975725000	-1.693373000	-0.912714000
1	6.173330000	-0.695744000	-1.072948000
7	-2.358560000	1.735131000	-0.815322000
7	-2.964844000	-1.311299000	0.579114000
7	-0.062123000	0.467194000	1.469277000
7	-0.029336000	-0.838024000	-1.358379000
8	3.139128000	-0.055472000	0.044570000
3	1.229999000	-0.113897000	0.043577000
21	-1.554697000	0.016628000	-0.059626000